Synthesis and Characterization of Zinc Oxide and Copper Doped Zinc Oxide Nanoparticles Using Orange Peel (*Citrus-sinensis*) Extract for Removal of Lead Ion from Waste Water

Zufan Gebrekidan Hadgu

A Thesis Submitted to the Department of Applied Chemistry

School of Applied Natural Science

Presented in Partial Fulfillment of the Requirements for the Degree of Master of Science in Chemistry (Industrial Chemistry)

Office of Graduate Studies

Adama Science and Technology University

September 2024

Adama, Ethiopia

Synthesis and Characterization of Zinc Oxide and Copper Doped Zinc Oxide Nanoparticles Using Orange Peel (*Citrus-sinensis*) Extract for Removal of Lead Ion from Waste Water

Zufan Gebrekidan Hadgu

Advisor: Dr Dereje Tsegaye

Co – Advisor: Dr Buzuayehu Abebe

A Thesis Submitted To the Department of Applied Chemistry

School of Applied Natural Science

Presented in Partial Fulfillment of the Requirements for the Degree of Master of Science in Chemistry (Industrial Chemistry)

Office of Graduate Studies

Adama Science and Technology University

September 2024

Adama, Ethiopia

Declaration and Recommendation

Declaration

I declare that this Master's Thesis entitled "Synthesis and Characterization of Zinc Oxide and Copper Doped Zinc Oxide Nanoparticles Using Orange Peel (*Citrus-sinensis*) Extract for Removal of Lead Ion from Waste Water" is my own work and has not been submitted to any university for similar purpose. The references used in this Thesis are duly recognized by proper citations.

Zufan Gebrekidan _____ _____

Name of student Signature Date

Recommendation

I/We, the advisor/s of this Thesis, hereby certify that I/we have read the revised version of this thesis entitled "Synthesis and Characterization of Zinc Oxide and Copper Doped Zinc Oxide Nanoparticles Using Orange Peel (*Citrus-sinensis*) Extract for Removal of Lead Ion from Waste Water" prepared under our guidance by **Zufan Gebrekidan Hadgu** Submitted in partial fulfillment of the requirements for the Degree of Mater of Science in Chemistry (Industrial Chemistry). Therefore, we recommend the submission of the revised version of the thesis to the department following the applicable procedures.

Dr Dereje Tsegaye	_____	_____
Advisor	Signature	Date
Dr Buzuayehu Abebe	_____	_____
Co-Advisor	Signature	Date

Approval Page

I/We the Advisors of the thesis entitled "Synthesis and Characterization of Zinc Oxide and Copper Doped Zinc Oxide Nanoparticles Using Orange Peel (*Citrus-sinensis*) Extract for Removal of Lead Ion from Waste Water" and developed by **Zufan Gebrekidan Hadgu**, hereby certify that the recommendation and suggestions made by the board of examiners are appropriately incorporated into the final version of the thesis.

Dr Dereje Tsegaye	_____	_____
Advisor	Signature	Date
Dr Buzuayehu Abebe	_____	_____
Co-Advisor	Signature	Date

Approval of Board of Examiners

We, the undersigned, members of the Board of Examiners of the thesis by **Zufan Gebrekidan Hadgu** have read and evaluated the thesis entitled "Synthesis and Characterization of Zinc Oxide and Copper Doped Zinc Oxide Nanoparticles Using Orange Peel (*Citrus-sinensis*) Extract for Removal of Lead Ion from Waste Water" and examined the candidate during the open defense. This is, therefore, to certify that the thesis is accepted for partial fulfillment of the requirement of the Degree of Master of Science in Chemistry (Industrial Chemistry).

_____	_____	_____
Chairperson	Signature	Date
_____	_____	_____
Internal Examiner	Signature	Date
_____	_____	_____
External Examiner	Signature	Date

Final approval and acceptance of the thesis are contingent upon the submission of its final copy to the Office of Postgraduate Studies (OPGS) through the Department Graduate Council (DGC) and School Graduate Committee (SGC).

_____	_____	_____
Department Head	Signature	Date
_____	_____	_____
School Dean	Signature	Date
_____	_____	_____
Office of post graduate Studies, Dean	Signature	Date

ACKNOWLEDGEMENTS

First let me start my thanks and glory to my GOD for providing me hope, health and strength throughout my work.

I would like to express my gratitude to my advisor Dr Dereje Tsegaye for his valuable advice, helpful discussions, devoted support and guidance. I also would like to express my special thanks and appreciation to my Co-Advisor Dr Buzuayehu Abebe whose guidance, support and encouragement has been precious throughout this study.

I would like to extend my sincere thanks to my supportive and encouraging husband Mr. Shishay Alem, for always believing in me and for the material assistance and moral support.

My heartfelt appreciation and honor also go to my work place Horticoop Soil and Water Analysis Laboratory, Bishoftu for providing me the laboratory service to do all my experiments. And I would like to express my deepest gratitude to Mr Ytbarek Tsegaw (Horticoop manager) for providing me unrestricted permission to do all my experiments, this research would not have been possible without his support.

Finally, my thanks go to Adama Science and Technology University, Department of Chemistry, for various supports and to all who directly and indirectly participate in the work.

Table of Contents

List of Figures

List of Tables

ACRONYMS AND ABBREVIATION

ACRONYMS

BLRV Blood Level reference value

CSD Chemical solution deposition

DMSO Dimethyl sulfoxide

DRs Diffuse reflectance spectroscopy

FTIR Fourier Transform Infrared spectroscopy

LED Light Emitting Diode

ICP- OES inductively coupled plasma optical emission spectrophotometer

JCPDS Joint Committee on Powder Diffraction Standards

MONPs Metal Oxide Nanoparticles

NPs Nanoparticles

PL Photoluminescence

SCS Solution combustion synthesis

SEM Scan Electron Microscopy

UV Ultraviolet Visible

XRD X-Ray diffraction

ABBREVIATIONS

CDC Center of disease and control

IARC International agency for research on cancer

IQ Intelligence quotient

US – EPA United state environmental protection agency

WHO World health organization

Abstract

The aim of this study was to synthesize pure and Cu doped ZnO Nanoparticles by using orange fruits peel (Citrus – sinensis) extract and metal precursor with solution combustion synthesis method and then to explore the capability of NPs as adsorbent for Pb^{2+} ion eradication from aqueous media by batch adsorption method. To confirm the synthesis all of the NPs were characterized using X-ray diffraction (XRD) spectroscopy, Fourier Transform Infrared (FTIR) spectroscopy, Scanning Electron Microscopy (SEM), Ultraviolet- Diffuse reflectance (UV- DRs) spectroscopy, and Photoluminescence (PL). The XRD result revealed that the phase structure of ZnO was wurtizite with crystallite size of 11.78, 11.61, 15.38, 20.43 and 27.78 nm for pure, 2%, 5%, 10% and 15% Cu doped ZnO NPs, respectively. UV-vis DRs confirmed band gap energy of synthesized NPs was found to be 3.24 and 3.16 eV for both pure and 15% Cu doped ZnO NPs from direct transitions, respectively. Adsorption potential of the synthesized NPs, towards Pb^{2+}, was also investigated. The influence of important factors affecting the adsorption process was determined, including the pH value(2 – 11), contact time(10 – 110 minute), nano adsorbent dose(0.025 g – 0.16 g) and the initial metal ion concentration(1 mg/L – 60 mg/L) to optimize the conditions. The concentration of Pb^{2+} ion was measured on ICP-OES at recommended wave length 220 nm. The Removal efficiency for waste water concentration (1.34 mg/L) of pb^{2+} ion solution was 83.9 % and 88.8 % for the pure and 2 % copper doped ZnO NPs. The adsorption reaction rate was examined by comparing Pseudo first order and Pseudo second order templates. From the observed result the adsorption reaction of Pb^{2+} ion on the NPs was fitted Pseudo second order template. Freundlich and Langmuir isotherm models were used to evaluate the sorption of Pb^{2+} ion on to the sorbent. Based on the models fitting value the preferential isotherm value for Pb^{2+} ion adsorption on ZnO-NPs was the Freundlich model signifying chemisorption. ZnO-NPs have the potential to be used as an effective and promising adsorbent material for eliminating metal ions from water solutions.

Keywords: Green synthesis, solution combustion reaction, ZnO NPs, Doping, *Citrus-sinensis*, and adsorption

1. INTRODUCTION

1.1 Background of the Study

Water is a primary natural resource, basic need to human being and all forms of life. Utilization of this natural asset needs appropriate planning and developmental management to serve safe drinking water. Natural water contamination is a serious challenge both at local and global level. Human activities, advances in industry and agricultural process have greatly affected the quality of water resource by allowing the release of hazardous metal ions to the environment. Some of the hazardous metals are lead (Pb), mercury (Hg), chromium (Cr) cadmium (Cd), nickel (Ni) and arsenic (As), which are becoming severe environmental and public health problems. The metal ion enters to water from industrial activities such as metallurgy, automotive, chemical and petro chemical sectors. (Al-Mur, 2023).

Infants and children's are susceptible to lead (II) ion toxification which may range from raised hearing threshold to reduction of intelligence quotient (IQ) at low blood lead level. In many developing countries occupational lead exposure which is the primary to lead (II) ion exposure is not well regulated. for example in Ethiopia even though there are various activities ranging from small scale to large industrial activities which uses lead based raw material which may pose lead (II) ion toxicity to workers, there is no a designed regulations to the workers about lead (II) ion poisoning. Peoples working in battery manufacturing company, gas stations attendants, radiator repairer, lead product solders and welders have the possibility to expose to lead (II) ion, which may cause gradual health risks. Due to lack of awareness and no any regulations to the exposure even the workers eat, drink, chewing khat (*Catha edulis*) and smoke while they are working (Adela et al., 2012).

Plumbum (Pb) otherwise named as lead is a carbon group chemical element, and malleable metal categorized as heavy metal. Lead (II) ion toxicity can be differentiated as acute and chronic. Acute lead ion exposure mostly involves rapid onset nausea, headache, cognitive change and emotional disruption where by chronic exposure involves neurodegradation and psychiatric manifestation including depression, anxiety, irritability, fatigue, decreased processing speed and fine gross motor deficits. Lead (II) ion introduced into a body is

excreted in urine and from liver to bile. The remained lead ion may bind to red blood cells, distributed through the soft tissue of our body and accumulates in bone for 20 – 30 years. Upon body bone turn over the accumulated lead (II) ion will turn back to blood stream, damages our nervous system (Mason et al., 2014). According to the International Agency for Research on Cancer (IARC), lead (II) ion is a possible carcinogenic substance in humans. The regulatory limit of Pb (II) ion in drinking water according to United States Environmental Protection Agency (US EPA) is 15 ppb. The World Health Organization (WHO) recommended safe limits of Pb (II) ion in wastewater and soils used for agriculture are 0.01 and 0.1 ppm, respectively, (Kinuthia et al., 2020). Centers for Disease Control and Prevention (CDC) also uses a blood lead reference value (BLRV) of 3.5 micrograms per deciliter (µg/dL) to identify children with blood lead levels that are higher than most children's levels (State et al., 2022).

Their non-biodegradability makes efficient removal of heavy metals from aqueous system which is greater advantage. Waste water heavy metal removing methods are chemical precipitation, ion exchange, absorption, membrane filtration, adsorption, coagulation and flocculation. Among these waste water treatment strategies adsorption is the most productive because of fair cost, easy to operate, uses renewable materials, high recovery rate and do not lead to sludge production (Xin et al., 2018).

Green chemistry synthesis approach, using biological components such as cellulose, enzymes, polysaccharides, flavonoids, alkaloids, terpenoids, alcohol etc. are accountable for the bio reduction of metal salt to its elemental form (Negi et al., 2021). However, there is no report of research related to the green synthesis of pure and Cu doped ZnO NPs using orange peel as capping agent, and/or reducing agent and its application in waste water treatment. In this study, orange (*citrus –sinensis*) fruits peel extract was used as a reducing agent for the synthesis of pure and Cu doped ZnO nanoparticles. A huge amount of orange production (80 %) is consumed to orange derivative products and approximately 40–70 % of the consumed fruit is transformed into citrus peel waste. In order to avoid orange peel accumulation, which may cause environmental and economic concern, the waste must be processed properly (Pandey & Yadav, 2015). Green synthesized zinc oxide nanoparticles were chosen as nano adsorbents specific for its characteristics such as high surface area to volume ratio, surface alteration, biocompatibility, reversibility and relatively low cost, which have allowed them to gain increasing attention as effective adsorbents (Negi et al., 2021).

1.2 Statement of the Problem

Water is a major input (and widely used) in different industries and is also discharged from same in plenty amounts. The industries are supposed to have discharge treatment facilities and recycling mechanism to be environmentally benign and economical. But practically, as in case of Ethiopia, most factories are discharging their waste without any further treatment. Such untreated wastes result in contaminating the environment (largely water and soil) with heavy metals, toxic organic and inorganic salts. Lead (II) is renowned as hazardous toxic material to ecosystems and human health as well. Lead (II) entry to environment is from automobile fuel exhaust and through effluents discharged from industries such as metal plating, oil refining and battery manufacturing and enters into body through inhalation, ingestion and skin adsorption. Lead (II) ion can act as cumulative poison and may accumulate in bones, brain, kidney and muscles which may cause many health risks like anemia, Neurodegradation, kidney diseases, sickness and even death (Yarkandi, 2014) and (Samad et al., 2021). Therefore, it is inevitable to get rid of lead (II) ion from the environment.

Adsorption is found to be efficient and cost effective method for removal of heavy metals from water bodies. In most adsorption applications researchers are looking for materials with high adsorption capacity. With this respect, nano materials have found wide applications due to their high surface area and modifiable surface morphology. The main drawback in the synthesis of nanomaerials is the use of chemicals that may affect the environment. The exploration for adsorbents with high removal capacity, low operating cost, easy accessibility, minimum production of chemical and biological sludge as a best alternative for industrial wastewater treatment practice has inspired our group to do the current study.

Therefore, in this research it was planned to use pure and Cu-doped ZnO nanoparticles which were synthesized by proceeding green method using orange (*citrus - sinensis*) fruits peel extract as potential nano adsorbents for lead (II) ion removal.

1.3 Objectives of the Study

The following were the general and specific objectives of the study.

1.3.1 General Objective

The overall objectives of this study was to synthesize and characterize pure and Cu doped

ZnO nano particles using orange (*citrus- sinensis*) fruits peel extract for the removal of lead (II) ion from waste water.

1.3.2 Specific Objectives

i. To synthesize pure zinc oxide nanoparticles and copper doped zinc oxide nanomaterial.

ii. To characterize pure zinc oxide nanoparticles and copper doped zinc oxide nanomaterial using XRD, FTIR, SEM, PL and UV-Vis DRs spectroscopic techniques.

iii. To evaluate the effect of pH, contact time, adsorbent dosage and initial concentration of the lead (II) ion on the adsorption efficiency of pure and copper doped zinc oxide Nanoparticles.

iv. To determine the lead ion adsorption characteristics on green synthesized pure zinc oxide Nanoparticles.

v. To study the removal of lead (II) ion from waste water using the synthesized pure and copper doped zinc oxide Nanoparticles.

1.4 Significance of the Study

The greatest advantage of this Study is that the pure and Cu doped ZnO NPs was synthesized by a green process extraction method which is ecofriendly unlike the chemical synthesis methods and the produced adsorbent could be an alternative in waste water treatment approaches. Generally, this study delivered information regarding the application of ZnO nanoparticle and also provided the importance of doping copper to zinc oxide nanoparticles and its application for lead (II) ion removal from waste water by adsorption procedure.

The output of this study is believed to contribute to the industry, government, scientific community and local community. The industry, the government as well as the local community are going to be benefited from having/introducing an alternative heavy metal removal material that help keep the environmental pollution to a minimum. Furthermore, changing the orange peel waste to a valuable material for the synthesis process has also additional positive impact on the environment. The research methods and the findings may also encourage other researchers to identify gaps and involve in further research activities.

1.5 Scope of the Study

This research work was limited to green synthesis of pure and Cu doped ZnO nanoparticle using orange (*citrus-sinensis*) fruits peel extract and characterization of the nanoparticles using XRD, FTIR, SEM, PL and UV- vis-DRs spectroscopic techniques and evaluation of the efficiency of the NPs for removal lead (II) ion from waste water.

2. LITRATURE REVIEW

2.1 Nano Particles

''Nano'' is derived from Greek word for dwarf (Tambe Patil, 2015). Nanoparticles are particles within the nano scale size between 1-100 nm with a surrounding interfacial layer, which can produce from large number of metals like Zn, Ag, Au, Cu, Ti, and Pt. It has been produced employing a range of methods using bio organisms, such as plants, fungi, bacteria and algae. Synthetic techniques that employ nontoxic solutions like water and plant extract are widely used in biosynthesis procedures to synthesize metallic nano particles. The biosynthesis of metallic nano particles has gained significant importance in recent years compared to chemical synthesis because of avoiding the use of toxic chemicals in the synthesis protocol (Kusdianto et al., 2021). And it also has several other merits, such as being a single step method, nontoxic, ecofriendly, low in cost, ease of application and is carried out under normal conditions. Additionally these nanoparticles show compatibility for bio-medical and pharmaceutical applications.

Researchers are trying to synthesize Nano particles with new properties to increase the range of their applications; improving waste water management using Nano particles is one of the major focuses of nanotechnology. Generally various techniques are available regarding environmental decontamination like adsorption, precipitation, ion exchange, reverse osmosis, electrochemical treatment, membrane filtration, evaporation, flotation, oxidation and bio sorption processes are extensively used. Nano particles can penetrate easily, where micro particles cannot penetrate to the contamination zone, so that nano particles are the ideal adsorbent which are suitable for the removal of different kinds of heavy metals (Chavali & Nikolova, 2019).

2.2 Major Classification of Nanoparticles

The nanoparticles are classified into different types on the basis of morphology, size and shape. Some of the important classes of nanoparticles are mention blew.

2.2.1 Carbon-Based Nanoparticles

Different methods of synthesis have led to the development of a wide variety of carbon-based nanomaterials during the past few decades. As a result of their unusual shape and varied qualities, they have found application in many multiple sectors. Nanomaterials based on carbon have several potential uses, including storing and producing energy, treating water and wastewater, and biological applications. There are a number of

allotropic shapes that carbon can take. Diamond, graphite, and buckminsterfullerene are all examples of allotropes. Graphite possesses the highest thermodynamic stability among them all. Because of its high conductivity, it can be used in a variety of electronic applications, Catalysts including batteries, electrodes, solar panels, etc.

Graphite is made up of stacked sheets of grapheme which is a new type of carbon that consists of a single layer of atoms arranged in a honeycomb arrangement on a two-dimensional sheet. It is quite useful as a building block in the creation of other forms of carbon nanoparticles due to its high strength. Carbon nanotubes are another novel form of carbon (CNTs). Although CNTs, fullerenes, and graphene are all synthesized in different ways, their physical properties and chemical properties are connected (Chavali & Nikolova, 2019).

2.2.2 Fullerene

Nobel laureates H. W. Kroto, R. F. Curl and R. E. Smalley discovered fullerenes in the year 1985. The fullerene family includes a number of atomic clusters (Cn) where n > 20. Fullerene C60 is the most common fullerene having 60 carbon atoms. It is also known as bucky ball. It is spherical in shape. Each carbon atom is sp2 hybridized and are linked together by covalent bonds. All the carbon atoms located at the vertices of 20 hexagons and 12 pentagons. About 28 to 1500 carbon atoms form the spherical structure with diameters up to 8.2 nm for a single layer and 4 to 36 nm for multi-layered fullerenes (Kumari & Sarkar, 2021).

2.2.3 Ceramic nanoparticles

Ceramic nanoparticles are also known as nonmetallic solid. The ceramics nanoparticles are synthesized via heating or successive cooling. The ceramic nanoparticles may polycrystalline, amorphous, porous, dens or hollow form. The researcher focuses on these nano particles due to their wide application such as photode gradation of dye, photocatalysis, catalysis and imaging applications (Ijaz et al., 2020).

2.2.4 Organic nanoparticles

The organic nanoparticles include ferritin, micelles, den-drimers and liposomes. The organic nanoparticles are not toxic, biodegradable and some organic nanoparticles have a hallow sphere i.e. micelles and Liposomes. It is also familiar with name of nano-capsules which are heat and light sensitive. Organic nanoparticles are an ideal choice for drugs delivery due to these characteristics. Then nanoparticles are also widely used in target drug

delivery. The organic nanoparticles are also known as polymeric nanoparticles. The most known shape of organic or polymeric nanoparticles is nanosphere or nanocapsule. The matrix particles are former overall mass of which is solid and outer boundary of spherical surface adsorbs other molecules. In the later case, particles encapsulated the solid mass (Ijaz et al., 2020).

2.2.5 Inorganic nanoparticles

Inorganic nanoparticles are the particles that are not made of carbon. It includes metal and metal oxides. As compared with organic NPs in inorganic NPs enormous research and commercial investments has been made (Kumari & Sarkar, 2021).

2.2.5(a) Metal-Based Nanoparticles

Metal-based nanoparticles are synthesized to nanometric sizes using either destructive or constructive processes. The nanoparticles of nearly every metal are synthesizable. Metals such as aluminum (Al), cadmium (Cd), cobalt (Co), copper (Cu), gold (Au), iron (Fe), lead (Pb), silver (Ag), and zinc (Zn) are frequently employed in nanoparticle synthesis. Metal nanoparticles, due to their quantum effects and enormous surface-to-volume ratio, have outstanding ultraviolet-visible sensitivity, electrical, catalytic, thermal, and antibacterial properties. As a result of the lower particle size, there are many more atoms on the surface. The surface area to volume ratio of particles varies according to the shape and size of nanoparticles, which in turn affects properties such as the ultraviolet-visible sensitivity and conductivity.

The electronic energy levels, electron affinities, electronic transitions, magnetic characteristics, phase transition temperature, melting point, and affinities to polymeric, biological, and organic substances are only some of the many properties that are influenced by changes in the surface area. Nanoparticles acquire their charge through a combination of the Coulomb charging effects and the quantum size mechanisms. There is a wide spectrum of intriguing properties obtained when the Coulomb charge effect is combined with the quantum size, which are not seen in the same bulk material. Particles with sharp edges and spherical shapes are particularly susceptible to quantum phenomena. Nanoparticles are used in catalysis, sensing, and imaging according to their size-dependent effects (Ijaz et al., 2020).

2.2.5 (b) Metal Oxides Nanoparticles

The engineered metals oxides nanoparticles (MONPs) are among the widest used manufactured nano materials because of their unique properties. The properties that make the nano phase structures indispensable tools in modern nanotechnology are their various nonlinear optical properties, higher ductility at elevated temperature, super paramagnetic behavior, unique catalytic, sensitivity and selective activity (Chavali & Nikolova, 2019).

Metal based NPs can be converted into their corresponding oxides known as metal oxides-based NPs. Some examples of metal oxides based NPs are Iron oxide (Fe_2O_3), Magnetite (Fe_3O_4), Aluminum oxide (Al_2O_3), Cerium oxide (CeO_2), Silicon dioxide (SiO_2), Titanium oxide (TiO_2), Zinc oxide (ZnO). These metal oxides based NPs found to be more reactive and efficient (Kumari & Sarkar, 2021).

2.3 Zinc Oxide Nanoparticles

Zinc oxide is an inorganic compound with formula ZnO, it usually appears as a white powder, as indicated in Table:1 ZnO owns unique physical and chemical properties (Vaseem et al., 2010). In addition ZnO has unique properties such as, high chemical stability, high electrochemical coupling coefficient, broad range of radiation absorption, high photo stability and is a multifunctional material (Ghorbani et al., 2015). Zinc oxide has appeared to be a prominent catalyst as far as water decontamination is concerned; on accounting that produces H_2O_2 more efficiently and shows high reaction and mineralization rates (Ali et al., 2013). The unique optical and electrical properties of ZnO nanoparticles such as wide band gap of 3.37 eV, large exciton band energy of 60 meV and high electron mobility at room temperature makes it suitable for new application and devices. Nanostructures ZnO have many potential application in photo catalysis, solar cell, gas sensors, fuel cells, photovoltaic antibacterial action and so on (Labhane et al., 2015). Applications of zinc oxide in various sectors are determined by the nanostructure of zinc oxide, which can be classified in to one-dimension (1D), two dimensions (2D) and three Dimensions (3D). One dimensional ZnO include nano rods, nano fibers, nanowires, nanotubes and nanoneedles. While, two-dimension ZnO and three Dimension ZnO are nano sheets and nano fibers, respectively (Kusdianto et al., 2021).

Table 1 Properties of Zno (Vaseem et al., 2010).

Properties	Values
Crystal Sturacture	Rock salt, Zinc blende and Wurtzite
Energy Band gap, meV	3.2 -3.3
Electron Mobilty,cm^2Vs^{-1}	2.5 – 300 Bulk ZnO, 1000 single nanowire
Exciton binding energy, meV	60
Density, g/cm^3	5.606
Refractive Index	2.0041
Electron Effective mass (me)	0.26
Relative Dielectric Constant	8.5
Melting Point, ^oC	1975
Boiling point, ^OC	2360
Electron Diffusion Coefficient cm^2s^{-1}	5.2 Bulk ZnO,$1.7x10^{-7}$(Particulate Film)

2.3.1 Copper Doped Zinc Oxide Nano Materials

To meet the requirement of different applications, the optoelectrical characteristics of the ZnO can be manipulated to attain preferable value by introducing an element impurities as a dopant into ZnO lattice site such as aluminum (Al), silver (Ag), copper (Cu) and tin (Sn). Through doping, the fundamental electrical and electronic characteristics of ZnO can be controlled which is the most significant issue in the development of optoelectronic devices and active electronics. Among the available dopants, Cu has identical electronic shell configuration and radius with Zn, making Cu a suitable dopant in the modification of ZnO optoelectronic properties (Labhane et al., 2015). The photo catalytic activity of ZnO can be enhanced by intensifying the surface charge transfer and/or decreasing recombination of electron and hole. Several methods to reduce electron hole recombination and amplify the surface charge transfer have been applied. One of these methods is the doping of transition metal in to ZnO. The doping of transition metal in to the ZnO lattice can lead to the change in the electrical, optical and magnetic properties. Besides, it reduces band gap energy of ZnO, amplify charge separation between electron and hole and enhance the photo catalytic activity (Molla et al., 2019).

As a result of transition metals doping, the surface of these NPs are transformed to exhibit greater feature such as a large surface-to-volume ratio and compact size, allowing them to

actively take part in photo catalysis and other applications. Cu^{2+} is reported to influence the structural, electrical, optical, biological and magnetic aspects of the ZnO NPs more than any other dopants. Cu^{2+} is the greatest alternative for biomedical applications because of its non-toxicity and its less ionic radii (0.073 nm) that is comparable to that of Zn^{2+} (0.074 nm). By incorporating Zn in to a CuO crystal structure or Cu in to a ZnO crystal structure, the combined dye degradation capabilities of ZnO and CuO can be explored. Furthermore, the doping process results in greater electrical conductivity to the dopants. It can quickly adjust or modify the ZnO's physical and chemical properties. Likewise Cu-doped ZnO NPs boost the storage capacity and energy conversion efficiency of electrochemical cells (Khalid et al., 2022).

2.4 Synthesis of Nanoparticles

Nanotechnology is the construction and utilization of functional structures designed from atomic /molecular scale and with at least one of its characteristics dimensions in nanometers by the use of numerous techniques. These techniques are generally categorized in to the bottom-up and top –down processes. In the bottom–up method nano size assemblies have been formed via means of molecular components. Whereas, with the top–down method, nanoparticles are generated from their constituent metals with help of the reserved microscopic device and transformed in to nano scale dimension (Patil et al., 2021).

2.5 Synthesis of ZnO Nano Particles and Cu- Doped ZnO Nano Materials

There are three kinds of approaches for the production of ZnO Nano particles.

These methods are

1. Physical methods 2. Chemical methods 3. Biological methods (Kusdianto et al., 2021).

2.5.1 Physical Methods

2.5.1.1 Gas Condensation

In this technique, a metallic or inorganic substantial is evaporated using thermal evaporation sources as like a Joule heated intractable containers, electron ray evaporation strategies, in an atmosphere of 1-50 mbar. Herein, a high stable gas pressure causes the creation of ultrafine elements (100 nm) by gas phase collision. Thus, very small particles are formed by impact of evaporated atoms with residual gas molecules. For this procedure, gas pressure should be greater than 3 MPa. Vaporization sources may be resistive heating,

high energy electron beams, low energy electron beam and inductive heating (Patil et al., 2021).

2.5.1.2 Vacuum Deposition and Vaporization

In vacuum deposition process, elements, alloys or compounds are vaporized and deposited in a vacuum. The vaporization source is the one that vaporizes materials by thermal processes. The process is carried out at pressure of less than 0.1 Pa (1 mTorr) and in vacuum levels of 10 to 0.1 MPa. The substrate temperature ranges from ambient to 500^{o}C. The saturation or equilibrium vapor pressure of a material is defined as the vapor pressure of the material in equilibrium with the solid or liquid surface. For vacuum deposition, a reasonable deposition rate can be obtained if the vaporization rate is high. A useful deposition rate is obtained at a vapor pressure of 1.3 Pa (0.01 Torr).Vapor phase nucleation can occur in dense vapor cloud by multi body collisions, the atoms are passed through a gas to offer necessary collision and cooling for nucleation. These particles are in the range of 1 to 100 nm and are called ultrafine particles or clusters (Patil et al., 2021).

2.5.2 Chemical Methods

Chemical synthesis methods are versatile in designing and synthesizing new materials that can be refined in to final product.

2.5.2.1 Precipitation Method

There are some techniques to synthesize ZnO-NPs. One of these is precipitation technique, which have many advantages i.e. more controllable, reproducible and the size of the particle obtained can be controlled easily. Below are some examples of precipitation synthesis methods.

2.5.2.1 (a) Modified Emulsion Precipitation Method

This method offers the advantage of avoiding agglomeration of the particles formed in the individual bubbles. This in turn makes possible later processing routes at unusually low temperatures. To take full advantage of the method for multi component oxides precipitation routes need to be designed so that an intimate mixture of atoms is formed during precipitation and chemical homogeneity is kept during later processing. This offers special challenges since emulsion co-precipitations tend to be carried out with sample precursors that do not affect emulsion stability but generally show a tendency to precipitate at different rates leading to at least partial phase segregation. This method involves the preparation of thermally stable emulsion systems prepared by adding proper amounts of

surfactants to a water oil system. Within the emulsion system, there are a small number of atoms per droplet. It is necessary that exchange of reactive species take place between droplets to form a stable precipitate.

From the Einstein Smoluchowski equation, the normal rate of the particle growth is faster than the equivalent rate of exchange between droplets. Therefore, the nucleation and growth in emulsions are retarded in comparison to those in homogeneous solution, avoiding the formation of large particles. Multi surfactants are effective in forming thermally stable emulsion and controlling droplet size. Other additives play a role as steric particle stabilizer after removal of water. Before the particle dispersion by filtration of decantation of the organic phase, the emulsions were prepared by mixing the oil phase (Cyclohexane or n-heptane) with tergitol surfactants and octan-1-ol as co surfactant. To the system stoichiometric amounts of water were added followed by vigorous mixing until a translucent emulsion was formed. The emulsion was added drop wise to alcohol solutions of alkoxides and stirred for several hours. After removal of solvents in dispersion the residue was taken up in acetone to destroy the micelles. The solid product obtained after decantation of the organic phase was dried and transformed to nano crystalline spinel's after calcinations (Yadav, 2017).

2.5.2.1 (b) Hydrothermal Synthesis/Solvothermal Synthesis

In this process, the chemical reaction takes place in a sealed vessel such as bomb or autoclave, where solvent are brought to temperature well about their boiling point. When water is used as solvent it is called a hydrothermal process. There are many advantages in using super critical condition such as simplicity, very low gain size, presence of a single phase and synthesis of high purity nano crystals with high crystalinity and eco friendliness nature. Solvothermal is synthesis technique of crystalizing substances from high temperature aqueous solutions at high vapor pressure (3Mpa) (Yadav, 2017).

2.5.2.1(c) Sol –Gel Method

The sol-gel process, also known as chemical solution deposition (CSD), is a wet chemical technique widely used in the fields of materials science and ceramic engineering. Such methods are used primarily for the fabrication of materials (typically a metal oxide) starting from a chemical solution (or sol) that acts as the precursor for an integrated network (or gel) of either discrete particles or network polymers. Typical precursors are metal alkoxides and metal chlorides, which undergo various forms of hydrolysis and poly

condensation reactions. In this chemical procedure, the 'sol' (or solution) gradually evolves towards the formation of a gel-like diphasic system containing both the liquid and solid phases whose morphologies range from discrete particles to continuous polymer networks. In the case of the colloid, the volume fraction of particles (or particle density) may be so low that a significant amount of fluid may need to be removed initially for the gel-like properties to be recognized. This can be accomplished in any number of ways. The simplest method is to allow time for sedimentation to occur, and then pour off the remaining liquid. Centrifugation can also be used to accelerate the process of phase separation. Removal of the remaining liquid (solvent) phase needs a drying process, which is typically accompanied by a significant amount of shrinkage and densification (Yadav, 2017).

2.5.2.2 Solution Combustion Synthesis Method

Solution combustion synthesis (SCS) is a versatile, simple and rapid process, which allows effective synthesis of a variety of nano size materials. This process involves a self-sustained reaction in homogeneous solution of different oxidizers (e.g., metal nitrates) and fuels (e.g., urea, glycine and hydrazides). Depending on the type of the precursors, as well as on conditions used for the process organization, the SCS may occur as either volume or layer-by-layer propagating combustion modes. This process not only yields nano size oxide materials but also allows uniform (homogeneous) doping of trace amounts of rare-earth impurity ions in a single step. Among the gamut of papers published in recent years on SCS, synthesis of luminescent materials and catalysts occupy the lion share. The gas less combustion synthesis yields much coarser particles than solution combustion synthesis (Aruna & Mukasyan, 2008).

2.5.3 Biological Method

The biosynthesis of metallic nanoparticles has gained significant importance in recent years compared to chemical synthesis because of avoiding the use of toxic chemicals in the synthesis protocol, and it also has several other merits, such as being a single-step method, non-toxic, eco-friendly, low in cost, ease of application and is carried out under normal conditions. Additionally, these nanoparticles show compatibility for bio-medical and pharmaceutical applications. Furthermore, because metal nanoparticles have various physicochemical features, such as sensing, catalytic, antibacterial, antioxidant, magnetic and electronic properties, scientists have demonstrated an interest in their production using novel techniques (Kusdianto et al., 2021).

2.5.3.1 Green Synthesis Using Microbes

The microorganism mediated synthesis of nanoparticles offers particles of small size, high surface area to volume ratio, thermal, magnetic, catalytic and biological properties which pave the way to synthesize different metal and metal oxide nanoparticles successfully (Negi et al., 2021).

2.5.3.2 Green Synthesis Using Biomolecules

In the green synthesis method in which nano particles with biocompatibility are produced, these agents are naturally present in the employed biological organisms. Because of rapid development, affordable culturing costs, easy control and manipulation of growth environment, bacteria are clearly targets in the production of nanoparticles (Yadav, 2017).

2.5.3.3 Green Synthesis Using Plants

The use of plant extract is a promising technique for the easy synthesis of metallic nanoparticles using green methods. So, the extracts of many types of plants have been used in ZnO NPs synthesis in different works. From the phytochemical analysis of the extract, it can be observed that flavonoids, phenolic and other molecules, which are found in the extract of the plant may cause the reduction of zinc ions, and control the biosynthesized nanoparticles size, where the hydroxyl, carboxylic and amino groups of phenolic, flavonoids, alkaloids, proteins, etc. which exist in the extract of plant may link to the zinc surface and trigger the formation of ZnO NPs, which was also supported by FTIR analysis. C=C, C=O-C and C=O groups of heterocyclic compounds, as well as amide from proteins may behave as stabilizers (Kusdianto et al., 2021).

2.6 Orange (*Citrus-Sinensis*) Fruit

Orange juice is one of the most widely-consumed beverages in today's world. And hence, the cultivation of oranges has become a major industry and an important economic sector in the India, United States and most Mediterranean countries. A high percentage of orange production (80%) is used to manufacture derivative products and approximately 40– 70% of the processed fruits is transformed into citrus peel waste (Pandey & Yadav, 2015). In order to prevent problems related to the disposal of this product and environmental concerns, this waste must be properly processed.

Orange fruit is one of the most productive fruit in the world. Orange fruit peel, as the main by-product of citrus, is rich in a variety of natural anti-oxidants. Therefore, the extract of

orange peel is considered to be used as a stabilizer to prepare ZnO NPs (Doan Thi et al., 2020).

2.6.1 Organic Contents of Orange (*Citrus- sinensis*) Fruit Peel

Orange peel is by product during the processing of fruit and studies show that they are good sources of bioactive compounds. Every year a large amount of oranges byproduct wastes are formed. Phytochemical analysis of orange peel extract showed the presence of tannins, terpenoids, flavonoids and saponins in different methods of extraction (Gotmare & Gade, 2018).

2.7 Application of Metal Oxide Nanoparticles (MONPs)

Application of metal oxides can be expanded in to various domains. The unique chemical and physical properties of MONPs are attributed to the high density and limited size of corners and edges on their surface. Potential technological applications of metal oxide nanoparticles play a vital role attracting researchers with considerable interest from the fields of material chemistry, medicine, agriculture, information technology, biomedical, optical, electronics, catalysis, environment, energy, and gas sensors (Chavali & Nikolova, 2019).

2.7.1 Application of Zinc Oxide and Copper Doped Zinc Oxide Nanoparticles

Researchers have shown interest in ZnO NPs in recent years because of their unusual chemical and optical properties. ZnO NPs are nanoparticles that have been used in a wide range of cutting-edge applications such as sensing, catalytic activity, antioxidant activity, biology, environmental protection, cosmetics, electronics, communication and the pharmaceutical fields. Furthermore, ZnO NPs are of great utility in bio-applications such as bio-sensing, drug delivery, gene delivery and nano-medicine, in addition to their antibacterial, antifungal, anti-diabetic, and larvicidal activities (Kusdianto et al., 2021).

Due to its inexpensiveness, nontoxic and environmentally safe property, ZnO has attracted more attention over last few years. Recently, modified ZnO was prepared by doping with transition metals such as Ag, Mn, Fe, Co, Cr, Al and Pd. The results of these transition metals doped ZnO show that the optical, magnetic and electrical properties changed with the change in concentration of transition metal. Electronic conductivity of Cu is very high and it is cheap and highly available on Earth's crust and so it is important metal for doping. The doping of Cu in ZnO is expected to modify absorption and other physical or/and

chemical properties of ZnO (Alahdal et al., 2022).Table 2 shows some of the applications of pure and Cu doped ZnO nano materials.

Table 2 Examples of various applications of pure and u doped ZnO NPs from published articles

Precursors	Calcinations Temperature and time	Technique	Morphology	Product	Polutant	Reference
$ZnCl_2$ and $CuCl_2$.2H2O	170°C/22hr	Hydrothermal	NPs	Cu doped ZnO	Methylene Blue	(Khalid et al., 2022)
Zn(OAc)2 .2H_2O	80°C/over night	Biosynthesis	NPs	ZnO	Cd and Pb	(Al-Mur, 2023)
Zn(CH3Coo)2	500°C/6hr	Combustion	NPs	ZnO	Dye degradation	(Ali et al., 2013)
$Zn(CH_3COO)_2$ $Cu(CH_3COO)2$ .H_2O	450°C/ 8hr	Co-precipitation	NPs	Cu doped ZnO	Dye degradation	(Labhane et al., 2015)
Zn $(NO_3)2$. 2H_2O	500°C/3h	Solution combustion synthesis	NPs	ZnO	Pb	(Godwin, 2022)
Zn $(NO_3)2$. 2H_2O	600°C/4hr	-	NPs	ZnO	Pb	(Samad et al., 2021)
Zn $(NO_3)2$. 2H_2O	400°C/2hr	Biological	NPs	ZnO	Photo catalysis	(Anbuvannan et al., 2015)
Zn and Cu salts	-	Chemical Co precipitation	NPs	ZnO	-	(Sajjad et al., 2018)
$ZnSO_4$and CuSO4	80°C/4hr	Hydrothermal	NPs	Cu doped ZnO	-	(Ben Saad et al., 2019)

2.7.1.1 Photo Catalytic Dye Degradation Applications

Zinc oxide is a potential photo catalytic material with band gap 3.4 eV, as a result of transition metal doping, the surface of these NPs are transformed to exhibit greater features such as a large surface area to volume ratio and compact size, allowing them to actively take part in photo catalysis and other applications. Cu^{2+} is reported to influence the structural, electrical, optical, biological and magnetic aspects of the zinc oxide NPs more than any other dopants. It is also observed that pure gold and silver doped ZnO NPs, synthesized by solution combustion method showed high photo catalytic efficiency on the degradation of methylene blue under UV exposure. The result was attributed to the noble metals clusters formed on the surface of ZnO nanoparticles during synthesis, which inhibited the recombination of the photo generated electron/hole pairs (Peng et al., 2019).

2.7.2.2 Anti-Bacterial Activities

A large number of materials which are considered to be safe develop toxicity at nano size range, which is mainly related to the increased surface area and high reactivity of nano size

materials and larger surface area (as in case of nanoparticles) ensures an increased range of probable interaction with bio-organics present on the viable cell surface. The considerable anti-microbial activities of inorganic metal oxides such as ZnO, MgO, TiO_2, SiO_2 and their selective toxicity to biological systems suggest the potential application as therapeutics diagnostics, surgical devices and nano medicine based antimicrobial agents. The advantage of using these inorganic oxide nanoparticles as antimicrobial agents are their greater effectiveness on resistant to strains of microbial pathogens, less toxicity and heat resistance. In addition, they provide mineral elements essential to human cell and even small amounts of them exhibit strong activity. ZnO nanoparticle has the potential to impact many aspects of food and agricultural systems because of its antimicrobial efficiency especially with the growing need to find alternative methods for formulating new type of safe and cost-effective antibiotics in controlling the spread of resisted pathogens in food processing environment (Emami-karvani & Chehrazi, 2012).

2.8 Waste Water Treatment

Into different bodies of water, such as rivers streams and seas, huge volumes of waste water are released. There are several organic and inorganic species in urban waste water. While the former contains sugars, lignin, fats, proteins, etc. arsenic, cadmium, chromium, copper, lead, mercury, zinc and so on are found in the later (Joshi & Shrivastava, 2011). The effect of their release into the environment is extreme and in turn impacts the food chain, and the sea life is directly impacted. It is therefore important to treat water prior to its release into the environment (Yusof & Hassan, 2020). Removal of wastes emitted from tanneries, electroplating systems, metal and wood processing industries is a prime necessity as discharge of untreated water results in serious environmental and public health problems.

In developing countries like Ethiopia pollution of water bodies from technological activities such as industrial effluents and agricultural chemicals is considered a minor threat, though urban water pollution is growing at alarmingly faster rates and the source are industries, municipal solid waste and oily wastes from garages and fuel stations (Mekonnen Engida & Xu, n.d.).

2.8.1 Removal Methods of Water Contaminants

The traditional methods, for the treatment of lead (II) ion and other toxic heavy metal contaminated wastewaters, include complexation, chemical oxidation or reduction, solvent

extraction, chemical precipitation, reverse osmosis, ion exchange, filtration, membrane processes, evaporation and coagulation. Besides the classical wastewater treatment techniques, adsorption of heavy metals is the most promising separation and purification method because this technique has significant advantages including high efficiency in removing very low levels of heavy metals from dilute solutions, easy handling, high selectivity, lower operating cost, minimum production of chemical or biological sludge and regeneration of adsorbent (Yarkandi, 2014).

2.8.2 Adsorption

Nano technology path ways, which are being employed for waste water treatment remediation, are due to its low cost, high performance, and ease of operation. The adsorption technology is considered to be the most promising way of extracting even trace quantities of heavy metal ions from effluents (Bercho, 2021). The basic principle of operation for adsorption is the mass transfer and adsorption of a molecule from a liquid or gas into solid surface. The substances that concentrate at the surface are called adsorbates and the material up on whose surface the adsorption takes place is called an adsorbent. The adsorbents should also have a pore structure which helps in fast transport of the gaseous vapors. The adsorbents categorized into one of three classes: as oxygen-containing compounds are typically hydrophilic and polar, including materials such as silica gel and zeolites, compounds of carbon-based are typically non polar and hydrophobic including materials such as activated carbon, graphite and polymer-based compounds are polar or non-polar functional groups in a porous polymer matrix (Gawande et al., 2017).

2.8.3 Zinc Oxide (ZnO) Nanoparticles for the Removal of Lead Ion from Waste Water

For the elimination of heavy metals, substantial investigations have been conducted concerning the creation of adsorbents such as polymer materials, activated carbons, biofuels, industrial byproducts and zeolites. Nonetheless, these adsorbents have substantial limitations, such as restricted loading capacities, few metal ion binding sites, low economic viability and poor selectivity. Considering these obstacles, scientists have concentrated on developing nano adsorbents for the elimination of contaminants from waste water. For the exclusion of heavy metals from industrial effluent, several nano-adsorbents (metal oxides) including ferric, manganese, aluminum, titanium, zinc, silicon, and selenium oxide nanoparticles have been developed. Metal oxides, such as ZnO, have long been predicted to be feasible nano adsorbents owing to their distinctive properties, such as their high

electron mobility, outstanding transparency, and robust room temperature luminescence. The unique physical, chemical and biological qualities of zinc oxide nanoparticles, such as their biocompatibility, environmental friendliness, inexpensiveness and non-toxic nature, make them one of the most significant metal oxide materials that have been extensively used in material research (Al-Mur, 2023).

The amounts of adsorption [q_e (mg/g)] at equilibrium and adsorption efficiency or percentage of removal (%) can be calculated by using the following expressions (Equations 1 and 2).

$$qe\,(mg/g) = \frac{(C_o - C_e)v}{m} \quad \text{---------- (1)}$$

$$\text{Removal efficiency, } \% = \frac{(C_o - C_e)}{Co} \times 100 \quad \text{---------- (2)}$$

where, C_o is the initial metal ion concentration and C_e is the final metal ion concentration, q_e is the amount of adsorbate adsorbed on the surface of the adsorbent, V is the volume of solution (L), m is the mass of adsorbent (g) (Kamath et al., 2019).

2.9 Parameters that Affect the Removal of Lead Ion by Adsorption

2.9.1 Effect of Initial Lead Concentration

The initial metal concentration is an important factor on the adsorption process since there are constant active binding site for a given mass of adsorbent where the fixed amount of metals can be adsorbed. Thus, increase in metal concentration in solution against same quantity of adsorbent, decreases the removal efficiency (Das & Rebecca, 2018).

2.9.2 Effect of pH

One of the effective factors that influence bio sorption of heavy metals in aqueous solution is pH. The hydrogen ion concentration affects solubilization and ionization of heavy metal ions in solution and present ionization state on adsorbent surface which determines the availability of metal active site (Das & Rebecca, 2018).

2.9.3 Effect of Contact Time

Contact time refers to the adsorption of the quantity of adsorbate by a definite quantity of sorbent with varying time span. The time factors in adsorption studies help to find out the equilibrium time of the process of adsorption (Samad et al., 2021).

Contact time is an important factor in batch adsorption process. The extent of metal removal was found to be increased first up of mixing and then the adsorption decreases. Initially the vacant surface sites are available for adsorption but they become saturated with the metal adsorption with the time. Moreover it would be difficult to be occupied due to repulsive forces between the bulk phases and the solute molecules on the solid (Kamath et al., 2019).

2.9.4 Effect of Adsorbent Dose

Adsorbent dose is vital parameter in adsorption studies as it helps to know the adsorption capacity of a particular sorbent against the metal ion solution at specific working conditions and as the quantity of adsorbent increases, the adsorption also increases (Samad et al., 2021).

The increment might be due to the larger surface area and availability of more adsorption sites, whereas the adsorption amount decreases with the adsorbent. This is because of the adsorptive capacity of adsorbent available was not fully utilized at a higher adsorbent dosage in comparison to lower adsorbent dosage (Kamath et al., 2019).

2.9.5 Adsorption Equilibrium Study

2.9.5.1 Langmuir Isotherm Model

Langmuir isotherm assumes monolayer adsorption onto a surface containing a finite number of adsorption sites of uniform strategies without transmigration of adsorbate in the plane surface. Once a site is filled no further adsorption can take at that site. This is indicative of the saturation point or the achievement of maximum adsorption by surface. The linear form of this isotherm is presented in Equation 3 (Kamath et al., 2019).

$$\frac{1}{q_e} = \frac{1}{q_m} + \frac{1}{q_m k_L C_e} \quad \text{---------- (3)}$$

Where, q_e is amount of metal adsorbed (mg/g), C_e is concentration after adsorption (mg/L), q_m is maximum monolayer coverage capacity (mg/g), K_L is Langmuir constant (L/mg). A linear plot of $(1/q_e)$ against $(1/C_e)$ with slope $(1/K_L q_m)$ and intercept of $(1/q_m)$ shows the satisfaction of the Langmuir model for adsorption. The constants K_L and q_m relate to the energy of adsorption and maximum adsorption capacity, respectively.

2.9.5.2 Freundlich Isotherm

The Freundlich model is based on the adsorption behavior of a heterogeneous surface in multilayer coverage. As per Freundlich model the stronger binding sites are occupied first followed by the weaker binding sites. The linear form of Freundlich isotherm model is given in Equation 4 as:

$$\log q_e = \log k_f + {}^{1}/_{n} \log C_e \text{---------- (4)}$$

Where, K_f is the Freundlich constant and the indicator of adsorption capacity whereas 1/ n is the strength of adsorption process or adsorption intensity. These constants are determined from the slope and intercept from the plot of log q_e (mg/g) against log C_e (mg/L). The value 'n' from this model indicates the degree of non-linearity between solution concentration and adsorption. According to literature, when n = 1, the adsorption is supposed to be of linear type and if it is more than 1, the adsorption is considered to be a physical process whereas it becomes chemical process when the value is less than 1 (Kamath et al., 2019).

2.9.6 Adsorption Kinetics Study

Kinetics of adsorption is one of the most important characteristic that is responsible for the efficiency of adsorbents. The adsorbate can be transferred from the solution phase to the surface of the adsorbent in several steps. In order to study the characteristics of the process and potential rate controlling steps, the kinetics of adsorption onto adsorbent can be analyzed by using different kinetic models. For such analysis, two kinetic models are widely applied. The kinetics of adsorption is analyzed by fitting the data into the Lagergrens first order model and pseudo second order equation to know the correlation coefficients (R^2). Pseudo-first order kinetics that generally describes the initial stage of the adsorption process is given in Equation 5 as:

$$\ln(q_{e-q_t}) = \ln(q_{e-k_1}t) \quad \text{or} \quad \log qe - qt = logq_{e-\frac{k}{2.303}t} \text{---------- (5)}$$

Similarly, the pseudo-second order kinetics, which provides better description of the whole adsorption process and based on the adsorption capacity, is expressed in Equation 6 as:

$$\frac{t}{qt} = \frac{1}{k_2 q_e^2} + \frac{t}{qe} \text{---------- (6)}$$

Where, q_e is the amount of material adsorbed ($mg.g^{-1}$) at equilibrium time and q_t is the amount of material adsorbed ($mg.g^{-1}$) at time t (min). k_1 and k_2 are the first order rate

constant (min^{-1}) and second order rate constant ($g.mg^{-1}.min^{-1}$), respectively. For first order kinetics, the value k_1 is obtained from the slope of the linear plot of log (q_e -q_t) against time (t) where the linear plot indicates the applicability of Lagergrens model. Similarly, for second order kinetics, the values of q_e and k_2 can be determined by the slope and intercept of the linear plot of t/q_t against time(t) (Kamath et al., 2019).

2.9.7 Common Characterization Techniques for Nanoparticles

Synthesis of nanoparticles needs to be validated by studying the different properties and characters of the synthesized materials. Commonly used characterization techniques are briefly discussed in this section.

2.9.7.1 X-ray Diffraction`

X-ray diffraction is now a common technique for the study of crystal structures and atomic spacing. X-ray diffraction is based on constructive interference of monochromatic X-rays and a crystalline sample. These X-rays are generated by a cathode ray tube, filtered to produce monochromatic radiation, collimated to concentrate, and directed toward the sample. The interaction of the incident rays with the sample produces constructive interference (and a diffracted ray) when conditions satisfy Bragg's Equation 7 as:

$n\lambda = 2d\sin\Theta$ ---------- (7)

Where n is an integer, λ is the wavelength of the X-rays, d is the inter planar spacing generating the diffraction, and Θ is the diffraction angle. This law relates the wavelength of electromagnetic radiation to the diffraction angle and the lattice spacing in a crystalline sample. These diffracted X-rays are then detected, processed and counted by scanning the sample through a range of 2Θ angles. X-ray diffraction is a high-tech, nondestructive technique for analyzing a wide range of materials including fluids, metals, minerals, polymers, catalysts, plastics, pharmaceuticals, thin-film coatings, ceramics, solar cells, and semiconductors (Bunaciu et al., 2015).

2.9.7.2 Fourier Transform Infrared Spectroscopy

FTIR is a powerfull and useful characterization methods for polymers and materials in general. This is an economic, short time characterization that allows to establish the chemical composition, microstructure, chemical interaction and even to follow variation of specific function groups with time, during reactions (Molla et al., 2019).

2.9.7.3 UV-VIS Diffuse Reflectance Spectrophotometry

The optical phenomenon known as diffuse reflectance is commonly used in the UV-visible, near-infrared (NIR), and mid-infrared (sometimes called drift or drifts) regions to obtain molecular spectroscopic information. It is usually used to obtain spectra of powders with minimum sample preparation. A reflectance spectrum is obtained by the collection and analysis of surface reflected electromagnetic radiation as a function of frequency (ν) usually in wave numbers (cm^{-1}) or wavelength (λ) usually in nanometers nm. Two different types of reflection can occur: regular or specular reflection usually associated with reflection from smooth, polished surfaces like mirrors and diffuse reflection associated with reflection from so called mat or dull surfaces textured like powders. The band gap energy (Eg) of ZnO can be obtained from the wavelength value corresponding to the intersection point of the vertical and horizontal part of the spectrum, using Equation 8.

$$E = \frac{hc}{\lambda} eV \quad \text{---------- (8)}$$

Where, E photon energy (eV), h is the Planck's constant (6.626 x 10^{-34} J s), C is the light velocity (3 x10^{8} m/s) and λ is the wavelength (nm).

The most often used theory to describe and analyze diffuse reflectance spectra is the Kubelka-Munk theory |Tuac equation. The two-constant Kubelka-Munk theory leads to conclusions that are qualitatively confirmed by experiment and can be used for quantitative determination of band gap energy of associated with direct transitions respectively as presented in Equation 9 (Sajjad et al., 2018).

$$F(R) = \frac{(1-R)^{1/2}}{2R} \quad \text{---------- (9)}$$

$$F(R) = \frac{(1-R)^{1/2}}{2R} \quad \text{---------- (10)}$$

Where R is the reflectance value and the band gap energy (Eg) of the sample was estimated from the variation of the Kubelka-Munk function with photon energy (Anbuvannan et al., 2015).

2.9.7.4 Scanning Electron Microscopy (SEM)

Scanning electron microscopy (SEM), can be regarded as an effective method in analysis of organic and inorganic materials on a nanometer to micro meter (µm) scale, it works at a high magnification reaches to 3,000,000x and even 10,000,000x (in some modern models) in producing images very precisely of wide range of materials (Mohammed & Abdullah, n.d.). The device allows analyzing samples with diameter up to 200 mm and height of 80

mm. Materials that can be used in SEM are organic and solid inorganic materials including metals and polymers. The morphology and structural organization of the prepared powder can be characterized by scanning electron microscopy (Mohammed & Abdullah, n.d.).

2.9.7.5 Photoluminescence

Photoluminescence (PL) spectra helped us to trace the fates of the photo generated electron/hole pairs. For effective photo catalytic reaction the photo generated electron/hole pair should follow the first path, thus, should not recombine. PL spectroscopy concerns monitoring the light emitted from atoms or molecules after they have absorbed photons. It is suitable for materials that exhibit photoluminescence. PL spectroscopy is suitable for the characterization of both organic and inorganic materials of virtually any size, and the samples can be in solid, liquid or gaseous forms. The sample's PL emission properties are characterized by four parameters: intensity, emission wavelength, bandwidth of the emission peak, and the emission stability (Gfroerer, 2006).

2.9.7.6 Determination of PH-Zero Charge of ZnO NPs

The pH point of zero charge (PZC) is the value of pH at which the components of surface charge are equal to zero for specified conditions of temperature, Pressure and aqueous solution components. The point of zero charge is also called the isoelectric point since the particles do not move when exposed to an electric field. It does not mean that there is no charge at the surface for pH of PZC, but there are equal amounts of both negative and positive charges. PZC is one of the essential features of the adsorption that greatly influence the percent of adsorption and is different from one material to another. Several methods have been developed to determine PZC in solution and other materials. One of them is salt addition or salt titration method (Adamu & Zereffa, n.d. & Cristiano, 2021).

3. MATERIALS AND METHODS

3.1 Chemicals and Reagents

Analytical grade chemicals and reagents including zinc nitrate hexa hydrate ($Zn(NO_3)_2.6H_2O$) (Central drug house (CDH), purity 99 %, India), copper nitrate tri hydrate ($(CuNO_3)_2.3H_2O$, (Lobachem, purity 95 %, India), buffer tablets ((with pH 4.0, 7.0 and 9.2) (Lobachem, India)), 1000 mg/L stock solutions of lead (II) ion (UNIChem chemical reagents, India) and distilled water without any further purification.

3.2 Apparatus and Instruments

The laboratory apparatus and equipment that were used during this research work were UV-Vis/DRS spectrophotometer (Shimadzu UV-3600 Spectrophotometer), X-ray diffraction spectrometer (XRD-7000S, Shimadzu, South Korea), FTIR spectrometer (Perkin Elmer's spectrophotometer, United states), Scanning Electron Microscope (JCM-6000plus Bench Top SEM, SHIMADZU Corporation, Japan), ICP-OES (FsH-12- 2010, Amytech, Germany), Photoluminescence (FLS 1000, Edinburgh Instruments UK), Analytical Balance (Adam 202,UK), oven (201-1AB, bench top equipment INC, India) beakers, Erlenmeyer flasks, test tubes, magnetic stirrer, thermometer, WhatmanNo.1filter paper, measuring cylinder, pH-meter (PH-16, PCE Industries, Germany), spatulas, volumetric flasks, ceramic crucibles, funnels, hot plate (Stuart 201, Germany) and muffle furnace (5x2-5-12G, Reagecon, Ireland) and bare magnets.

3.3 Experimental Methods

3.3.1 Preparation of Orange Peel

The orange (*Citrus-sinensis*) fruits were purchased from Bishoftu local market, Oromia Region, Ethiopia. The fruits were washed several times with tap water followed by distilled water to remove extraneous matters. The cleaned orange fruits were peeled off keeping as much as the white membranous part of the peel as possible, and the peel were washed with distilled water and dried in an oven at 65^{o}C for 12 hours, the dried peel were grinded to fine powder and stored properly for further usage.

3.3.2 Preparation of Orange Peel (*Citrus Sinensis*) Fruit Extract

The extraction of the fruit peel was carried out as follows. 3.00 gram of the orange fruit peel powder was weighed and mixed with 100 mL distilled water and stirred on magnetic stirrer for 3 hours. Then the mixture was heated on hot plate near to boiling for 1hour and

the boiled suspension formed in the solution was allowed to cool and was filtered using whatman filter paper and stored for further work (Doan Thi et al., 2020).

3.3.3 Preparation of Precursor Salt Solution

The preparation of 0.35 molar precursor salt was carried out by precisely weighing 2.603 gram zinc nitrate hexa hydrate (Zn $(NO_3)_2.6H_2O$) in to 25 mL volumetric flask and was dissolved in small amount of distilled water by slowly stirring, and then filled to 25 mL and stored for the next step.

3.3.4 Synthesis of Zinc Oxide Nanoparticles Using Orange (*Citrus sinensis*) Peel Extract

A facile solution combustion synthesis technique is used to synthesize ZnO NPs as reported in previous work (Ali et al., 2013) but modified by introducing plant extract as capping agent. 10 mL of 0.35 molar zinc nitrate hexa hydrate ($ZnNO_3.6H_2O$) were mixed with 20 mL fruit extract and were stirred for one hour on magnetic stirrer and the mixture solution was heated on hot plate near to boiling (Lucilha et al., 2014). The solution forms a yellowish jelly on heating. This yellowish jelly was combusted by further heating and a mixture of black and white powder was formed (ZnO as-synthesized). Further the synthesized powder was calicnated on a muffle furnace for three hours at 450^oC and white powder of ZnO was formed as shown in Figure 1 and stored for extra characterization and experimental use.

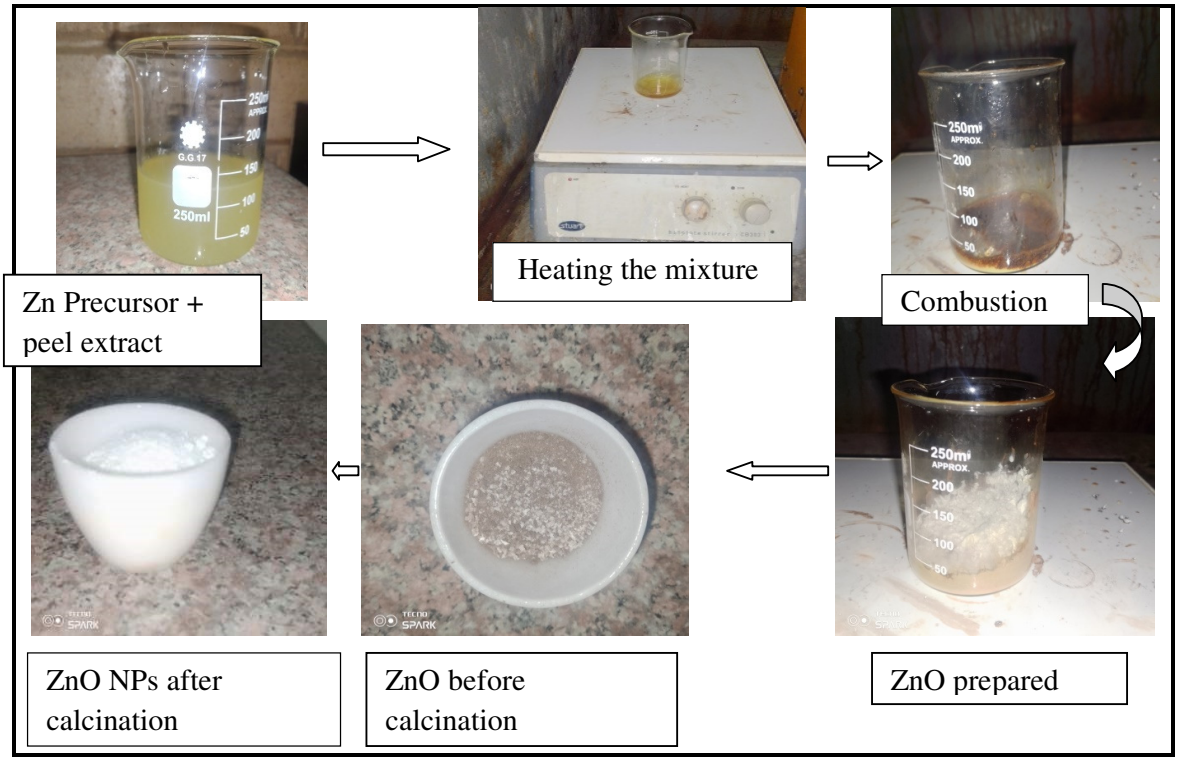

Figure 1 Schematic diagram for the synthesis procedure of ZnO NPs

3.3.5 Synthesis of Cu-Doped Zinc Oxide Nano Material

The Cu - doped ZnO nano material were also synthesized using the same approach as in Section 3.3.4, except the addition of 2, 5, 10 and 15 percent by weight of copper nitrate tri hydrate ($Cu(NO_3)_2.3H_2O$). Different amount of Cu were added into Zn precursor solution and the steps and procedures were the same as pure ZnO synthesis. The prepared copper doped nano materials were stored in a tightly closed jar for characterization and experimental use.

3.4. Characterization of Synthesized Pure and Cu Doped ZnO Nano Material

3.4.1 Characterization Using X-Ray Diffractometer (XRD)

The crystalinity, structure imperfections and average grain size of the synthesized pure and copper doped ZnO NPs were examined by using the Shimadzu XRD-7000S X-ray diffractometer (XRD) at Adama Science and Technology University Material Science and Engineering Department. The x-ray diffraction (XRD) patterns were recorded at the angel range of 2θ from 10^o up to 80^o using Cu Kα (λ = 1.5406 nm) radiation with an accelerating voltage of 40 kV. The crystallite size D of a particle can be estimated according to the Scherrer equation (Equation 11).

$$D = \frac{K\lambda}{\beta\cos\theta} \text{---------- (11)}$$

Where, K= shape factor, which is assigned a value of 0.94, λ= x-ray wave length (1.5421A^0), D is the average diameter of the crystals, β = full width at half maximum in radians and θ= Bragg's angle (Bunaciu et al., 2015).

Sample preparation and determination: about 0.5-1.5 gram of dried ZnO NPs grinded by mortar and pestle and then it was filled into the sample holder and subjected into X-ray diffractometer.

3.4.2 Characterization Using Fourier Transform Infrared (FTIR)

FTIR analysis of the synthesized nanomaterials was done at Bahir Dar University. FTIR spectrum of the calcinated powder of the green synthesized pure and Cu doped ZnO samples was recorded in the range 4000 - 400 cm^{-1}. FT-IR is used to identify the functional groups of the active components of pure and Cu doped ZnO NPs.

Sample preparation and determination: To create a very thin powder, the synthesized nanomaterial powders were combined with potassium bromide (KBr) powder. The powder mixtures were then squeezed under pressure to form thin pellets. A thin, transparent pellet made from the powder mixture was then utilized to record the FTIR spectrum.

3.4.3 Characterization Using UV-Vis DRs Spectrometer

Optical property of pure and Cu doped ZnO NPs synthesized by using orange peel extract was studied using Ultra violet- Visible DRs spectrometer with the adsorption range 200 nm – 800 nm at Adama Science and Technology University, Department of material science and Engineering.

The band gap energy (Eg) of pure and Cu doped zinc oxide was obtained from the wavelength value corresponding to the intersection point of the vertical and horizontal part of the spectrum, using the equation 9 and 10.

The most often used theory to describe and analyze diffuse reflectance spectra is the Kubelka-Munk theory |Tuac equation. The two-constant Kubelka-Munk theory leads to conclusions that are qualitatively confirmed by experiment and can be used for quantitative determination of band gap energy of associated with direct and indirect transitions respectively as presented in Equation 9 and 10 (Sajjad et al., 2018).

$$F(R) = \frac{(1-R)^2}{2R} \quad \text{----------} \quad (9)$$

$$F(R) = \frac{(1-R)^{1/2}}{2R} \quad \text{----------} \quad (10)$$

Where R is the reflectance value and the band gap energy (Eg) of the sample was estimated from the variation of the Kubelka-Munk function with photon energy (Anbuvannan et al., 2015).

Sample preparation and measurement: The powdered samples and finely grounded $BaSO_4$ standard were carefully filled to the sample holder and the diffuse reflectance is measured after the sample holder was positioned horizontally at the base of integrating sphere.

3.4.4 Characterization Using Scanning Electron Microscope (SEM)

SEM analysis of the green synthesized pure and Cu doped ZnO NPs was carried out by using SEM at Adama Science and Technology University, Biology Department, which reveals information about the surface morphology of the green synthesized pure and Cu doped ZnO samples with direct visualization.

Sample preparation and determination: A small amount of powder sample was placed in SEM chamber and creates a vacuum by evacuating air, the sample was scanned with electrons and image was captured.

3.4.5 Characterization Using Photoluminescence Analysis (PL)

PL analysis of the synthesized nanomaterials was done at Adama science and Technology University, Physics Department. PL spectrum of the calcinated powder of the green synthesized pure and Cu doped ZnO NPs samples were recorded on Photoluminescence. Photoluminescence (PL) spectra helped us to trace the fates of the photo generated electron/hole pairs (Gfroerer, 2006).

Sample preparation: both the synthesized pure and copper doped zinc oxide nanoparticles were dispersed in 10 mL Dimethyl sulfoxide (DMSO) solution and the intensity was measured using quartz cuvette with 1 cm path length.

3.5 Determination of pH of zero charge (PZC) for ZnO NPs

The pH of zero charge was determined by salt addition method using 0.1M KNO_3 solution and pH meter. 0.1M KNO_3 solution was prepares by weighing 10.11g KNO_3 and was

dissolved in 500 mL distilled water, in 1000 mL volumetric flask and finally filled to final volume using distilled water. 50 mL of KNO_3 was taken in to 250 mL flasks with different pH values (pH 2, 3, 4, 5, 6, 7, 8, 9, 10, 11 and 12) adjusted using 0.1M HCL and 0.1M NaOH, and then 0.08 g of ZnO NPs was added. The samples were then agitated at 150 rpm for 24 hours. Next day the samples were filtered and pH of the filtrate was measured using pH meter and the change in pH was calculated and the change in pH (Y-axis) was plotted against the initial pH (X-axis). This curve intersection with the initial pH is equal to change in pH is known as pH pzc.

3.6 Adsorption Study of Lead Ion by Synthesized Zinc Oxide Nanoparticles

3.6.1 Standard Working Solutions Preparation

1000 mg/L standard stock solution of lead (II) ion (UNIchem chemical reagents) was purchased from local chemical suppliers. 250 mg/L intermediate solution was prepared from the 1000 mg/L stock solution by appropriate dilution. The calibration series solutions, with different concentrations 1 mg/L, 5 mg/L, 10 mg/L, 20 mg/L, 30 mg/L, and 40 mg/L of lead ion were prepared by taking appropriate volume of the intermediate solution in 100 mL volumetric flasks by serial dilution process and used to instrument calibration and adsorption procedure.

3.6.2 Batch adsorption experiments

Batch adsorption experiments were carried out at room temperature. The solution pH was adjusted by using buffer tablets (pH 4.0, pH 7.0 and pH 9.2). The adsorption experiment was conducted by varying adsorbent dose (0.025 g – 1.6 g), Pb (II) ion concentration (1 mg/L– 60 mg/L), agitation time (10 min - 110 min) and pH (2, 4, 6, 7, 9 and 11).The solutions of Pb (II) ion prepared from the intermediate solution were taken into Erlenmeyer flasks. After pH was adjusted, a known quantity of adsorbent was added and finally, metal-bearing suspensions were kept under mechanical shaker. After shaking, the suspension was allowed to settle and the residual adsorbent with metal ions was filtered using Whatman filter paper, and metal ion concentrations in the filtrate were determined by ICP-OES spectrophotometer.

The amounts of adsorption [q_e (mg/g)] at equilibrium and adsorption efficiency or percentage of removal (%) were calculated by using Equations 1 and 2. This removal percentage and amount of adsorption were investigated for different parameters such as metal ion concentration, effect of pH, adsorbent amount and mixing time.

3.6.3 Adsorption kinetics Study

Adsorption kinetics is used to understand the adsorption mechanism and the effect of contact time. In this work the optimum values like 0.08 g pure and Cu doped ZnO NPs, 150 rpm agitation speed, pH=7.0 and 20 mg/L Pb (II) ion concentration were used to study the adsorption kinetics.10 mL of samples were taken after the following time intervals: 10 min, 30 min, 50 min, 70 min, 90 min and 110 min and sample were filtered to remove ZnO particles and then Pb (II) ion content was determined using plasma system (ICP-OES). Based on the results obtained and using Equations 5 and 6 the kinetics model was deduced.

3.6.4 Adsorption Isotherm of Lead Ion on Zinc Oxide NPs

The adsorption isotherm studies were obtained as follows, different known concentration of lead (II) ion like 1 mg/L, 10 mg/L, 20 mg/L, 30 mg/L, 40 mg/L, 50 mg/L and 60 mg/L were taken to different Erlenmeyer flasks and 0.08 g of pure and copper doped zinc oxide nanoparticles were added and put on an orbital shaker at 150 rpm for 50 min, the flasks were settled down for 30 min. samples were taken from the upper clear part of the solution and concentration of lead (II) ion in the solution was measured using ICP-OES.

3.6.5 Application of Green Synthesized Adsorbents to Removal of Lead Ion from Real Waste Water

Water sample was collected from garage waste (Bishoftu, Oromia, Ethiopia) immediately after the garage workers wash and clean the materials used/maintained. The collected sample was acidified with HNO_3 and stored in refrigerator until the analysis is done. The metal analysis of the sample was done after filtration through filter paper on ICP – OES and its pH on pH – meter. After adjusting its pH to 7.0 the sample was treated with pure and 2% Cu doped (selected due its relatively smaller size than others based on XRD result) ZnO NPs at optimum conditions of pH=7, agitation time 50 minute and calculated adsorbent dose (0.015g) from the optimization procedure. The ICP-OES was calibrated with the previously prepared calibration solutions and determination of lead (II) ion in the waste water was conducted after the adsorption process.

3.6.6 Statistical Analysis Using Student t-Test

From the triplicate data determination of Pb concentration after adsorption process of waste water on both pure and 2% Cu doped ZnO NPs the statistical analysis was done using student t- Test procedure. It was found that there is significant difference between pure ZnO and Cu doped ZnO NPs on the adsorption capacity of Pb (II) ion ($p< 0.05$) as shown in appendix.

4. RESULTS AND DISCUSSION

4.1 Characterization of Zinc Oxide Nano particle and Copper Doped Zinc Oxide Nano Material

4.1.1 X-ray Diffraction (XRD) Analysis

Phase purity and crystallinty of synthesized pure and copper doped ZnO nanoparticles were identified by XRD analysis at the 2Ɵ range of 20-80. Five samples were synthesized by 1:2 metal precursors to fruit peel extract ratio (pure ZnO, 2%, 5%, 10% and 15% Cu doped ZnO). The diffraction peaks were observed as presented in Figure 2 (a up to e) and Table 3 which correspond to the crystal plane of (100), (002), (101), (102), (110) (103) and (112).

The diffraction patterns of pure and copper doped ZnO NPs were found to be in good agreement with Joint Committee on Powder Diffraction Standards (JCPDS) card number 00-036-1451, which confirms the formation of pure ZnO NPs without the formation of any secondary phase. This implies that the green synthesized pure and copper doped ZnO nanoparticle possessed higher crystallinity, hexagonal (wurtizite) phase and no XRD detectable impurities, which confirm the purity of the pure and copper doped zinc oxide nanoparticles (Labhane et al., 2015).

The crystal size of the solution combustion synthesized pure and copper doped zinc oxide nano particles were calculated by Debye Scherrer Equation 11 and the crystal size corresponding to the three highest intense peaks were calculated and found to be as 11.78, 11.61, 15.38, 20.43 and 27.89 nm for the pure, 2 %, 5 %, 10 % and 15 % copper doped zinc oxide nanoparticles, respectively, (Table 3). The result showed that the plant extract was responsible for the reduction or/and capping of the metals to produce nanoparticle.

The average grain size of ZnO is reduced from 11.78 – 11.61 nm by the addition of 2% Cu, this is due to the inclusion of Cu in the host ZnO, which decreases the nucleation and subsequent growth rate by the addition of 2% Cu concentration. This conclusion is consistent with the report of (Sajjad et al., 2018). The grain size increment for the samples with 5 %, 10 % and 15% of Cu concentration with average grain size 15.38 nm, 20.43 nm and 27.89 nm, respectively, is due to the greater % copper causes more defects and deformed lattice structure. The presence of more defects greatly deteriorate the grain size and shape, hence the grain size and shape for greater than 5 % is larger than the pure and 2 % doped samples.

There is also a slight right peak shift observed which increases as the doping amount increases. This peak shift is due to the smaller size of Cu ion (0.073 nm) as compared to the host (0.074 nm) which decrease the inter planner space (d) (contraction/shrinkage will occur and a substitution doping is happened).

Table 3 Crystallite sizes of synthesized pure and copper doped ZnO NPs

Sample name	Peak position (2Ɵ)	FWHM (deg.)	Crystal size D(nm)	Average D (nm)
Pure ZnO	31.70	0.687	12.56	11.78
	34.32	0.758	11.46	
	36.14	0.772	11.31	
2% Cu doped ZnO	31.70	0.691	12.48	11.61
	34.35	0.790	11.00	
	36.15	0.769	11.35	
5% Cu doped ZnO	31.71	0.545	15.83	15.38
	34.36	0.562	15.46	
	36.18	0.588	14.85	
10 % Cu doped ZnO	31.68	0.418	20.64	20.43
	34.35	0.424	20.49	
	36.16	0.433	20.17	
15 % Cu doped ZnO	31.7	0.310	27.83	27.89
	34.36	0.314	27.67	
	36.18	0.310	28.17	

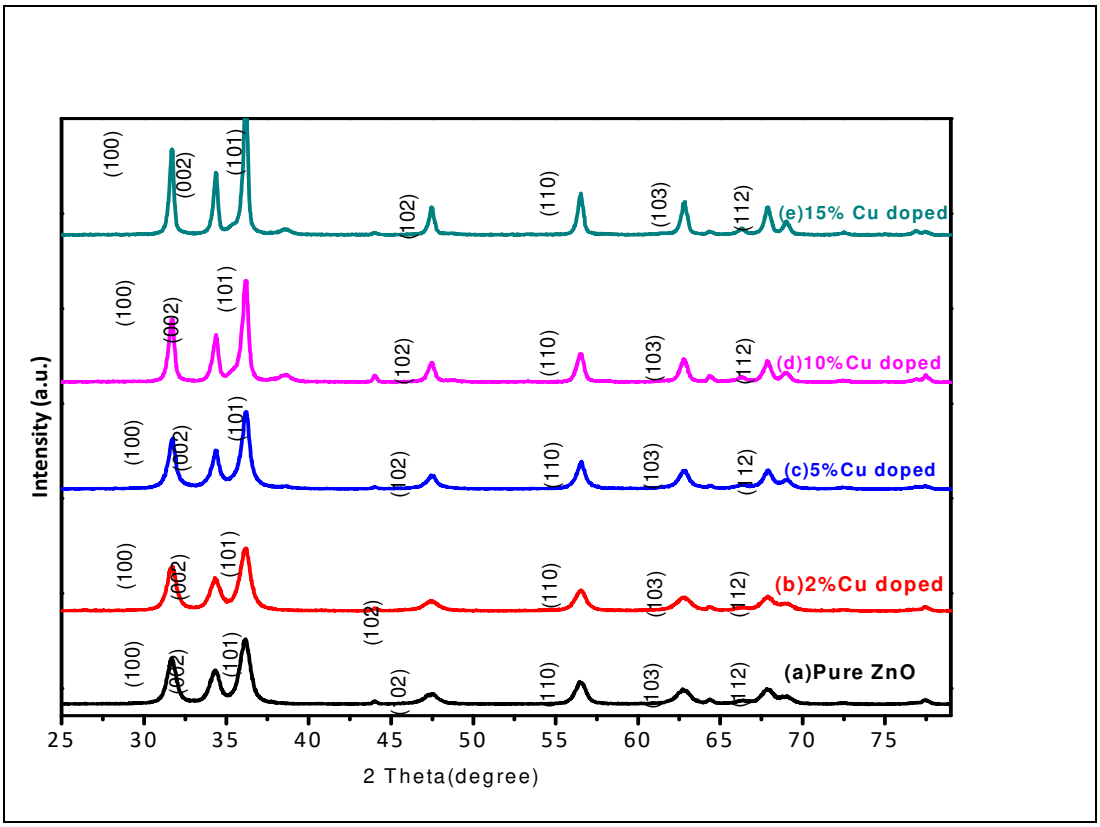

Figure 2 XRD Patterns of the green synthesized pure and copper doped ZnO NPS as (a) pure ZnO, (b)2% copper doped ZnO, (c) 5% copper doped ZnO, (d) 10% copper doped ZnO and (e) 15% copper doped ZnO NPs

4.1.2 FT-IR Analysis

FTIR spectra (transmittance vs wave number) of pure and Cu doped ZnO nanoparticles are shown in the Figure 3. FT-IR was performed in order to study and determine the functional groups of synthesized pure and copper doped ZnO nanoparticles. The analysis was done at a wave number range of 400 – 4000 cm^{-1}. Different peaks were observed at different wave number values. The strong wide band at around 3400 cm^{-1} is due to O-H stretching associated with the surface absorbed water molecule. The band appeared at 2400 cm^{-1} is due to the C-O stretching vibration, indicates the CO adsorption on the metal oxide surface. Similarly, the bands around 1400 cm^{-1} and 1100 cm^{-1} are due to CO_2 and M-O-O-M peroxide formation, respectively. The FTIR spectrum of the weak band around 690 cm^{-1} is due to M-O stretching of metal oxide and this is a perfect indicating for the ZnO matrix vibration and its synthesis (Labhane et al., 2015).

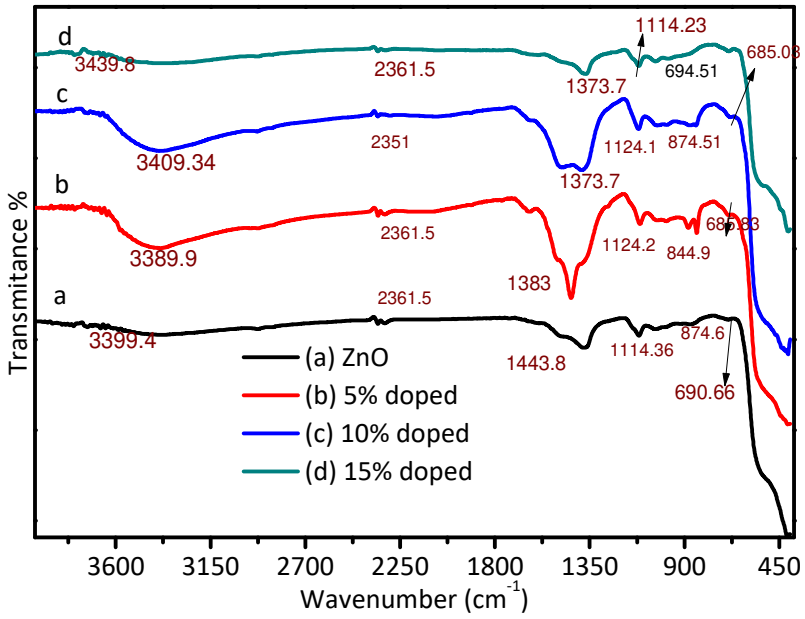

Figure: 3 FTIR spectrums of pure and copper doped Zinc oxide nanoparticles

4.1.3 Ultra Violet –Visible Diffuse Reflectance (UV-VIS DRs) Analysis

For band gap studies, Diffuse Reflectance Spectroscopy (DRs) technique was used. From DRs Spectra, the band gaps of pure and Cu-doped ZnO NPs were calculated after Kubelka–Munk treatment and Tauc's plot which is expressed in Equation 9 and 10.The sudden decrease of reflectance as shown in Figure 4 (A), at a particular wavelength, corresponding to the optical band gap means that the particles are almost uniformly distributed in the sample and it indicates absorption of light at that wave length. It is also suggested that the material has improved its absorption property which is important to some applications like catalysis. The band gap energy represents the minimum energy necessary to excite an electron. The energy band gaps of pure and Cu doped ZnO NPs were estimated using Kubelka–Munk plots. The energy band gap of pure and 15 % copper doped ZnO NPs were evaluated from $(F(R)*E)^{1/2}$ vs the photon energy (E) and $(F(R)*E)^{2}$ vs the photon energy (E) and as shown in Figure 4B and C by extrapolating the straight line to the x-axis. The direct band gap of pure and doped NPs was found to be 3.25 eV and 3.12 eV for direct transitions, respectively. The indirect band gap of pure and doped NPs was found to be 3.16 eV and 2.95 eV transitions, respectively. The band gap energy for the doped NPs is decreased to 2.95 eV), this red shift is caused by Cu doping in ZnO associated to the dopant-host sp-d exchange interaction (Sajjad et al., 2018).

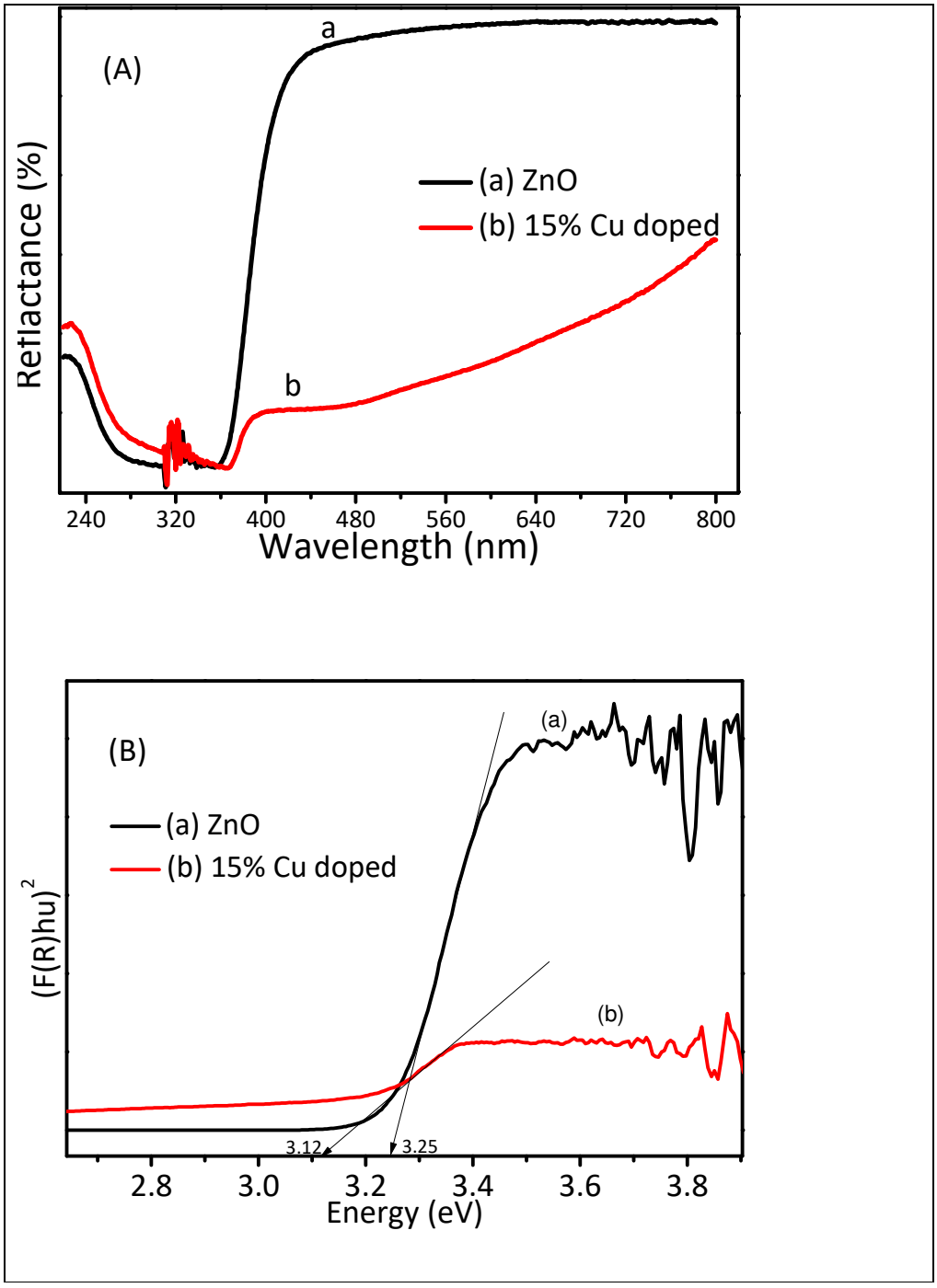
(A)
a
b
(a) ZnO
(b) 15% Cu doped
Retlactance (%)
240
320
400
480
560
640
720
800
Wavelength (nm)
(B)
(a) ZnO
(b) 15% Cu doped
(F(R)hu)2
(a)
(b)
3.12
3.25
2.8
3.0
3.2
3.4
3.6
3.8
Energy (eV)

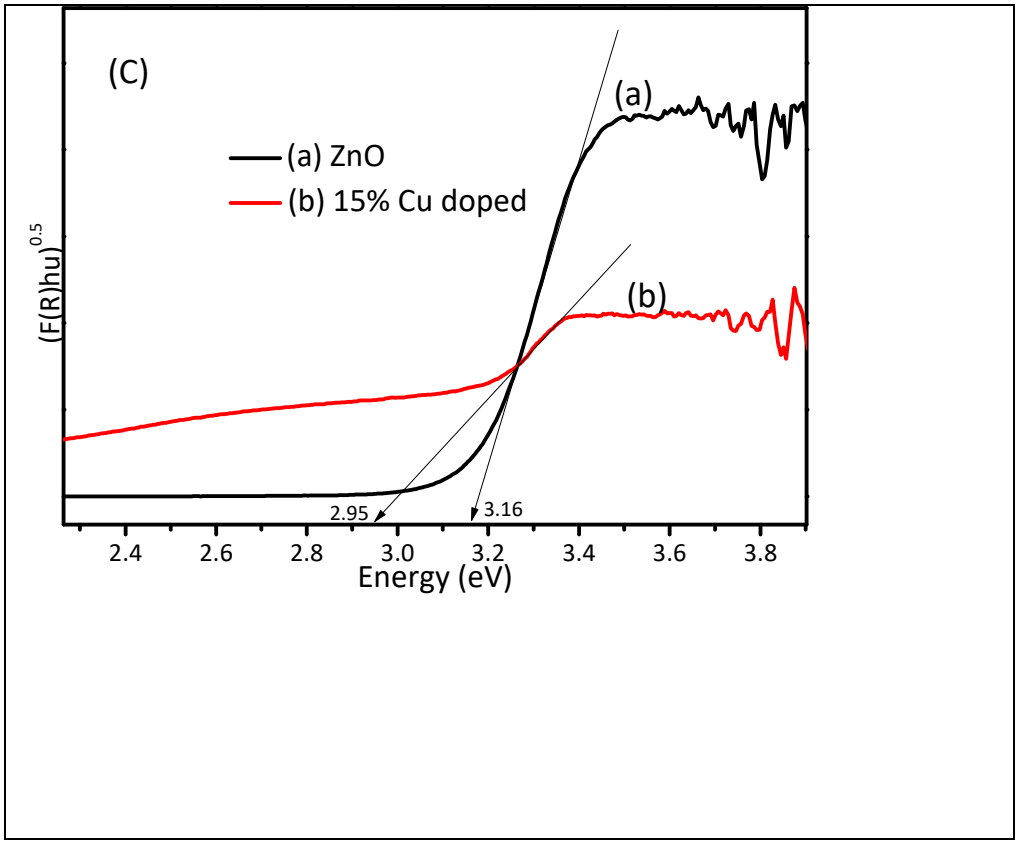

Figure 4. (A) DRS-UV-vis spectrum, (B and C) the direct and indirect Kubelka–Munk plots of green synthesized pure and 15 % doped with Cu-ZnO nanoparticles.

4.1.4 Photoluminescence (PL) Analysis

Photoluminescence analysis was done in order to investigate the optical property of ZnO and the effect of Cu doping on ZnO properties at room temperature. PL spectra of pure and Cu-doped ZnO with different amounts of Cu are illustrated in Figure 6. The pure ZnO have only one peak in the UV region (391 nm) and another visible region (414 nm) of the spectrum. The UV region peak corresponds to near band edge emission (NBE) which is due to exciton related transitions and visible region peak appears because of crystal defects like Zn interstitials and oxygen vacancies. On the other hand, when copper was incorporated to the structure, the UV peak was observed to be shifted towards comparatively larger wavelength (red shift) because of the change in electronic structure and that in the band gap of the doped structures. Upon doping, impurity states are created below the conduction band due to which red shift appears. In addition with increasing the Cu content besides the red shift, a change in intensity of the two peaks was observed. The intensities of UV and visible peaks was decreased as the amount of dopant increases

which, shows that the recombination rate of electrons and holes decreases which, is very important in improving the property of ZnO (Sajjad et al., 2018).

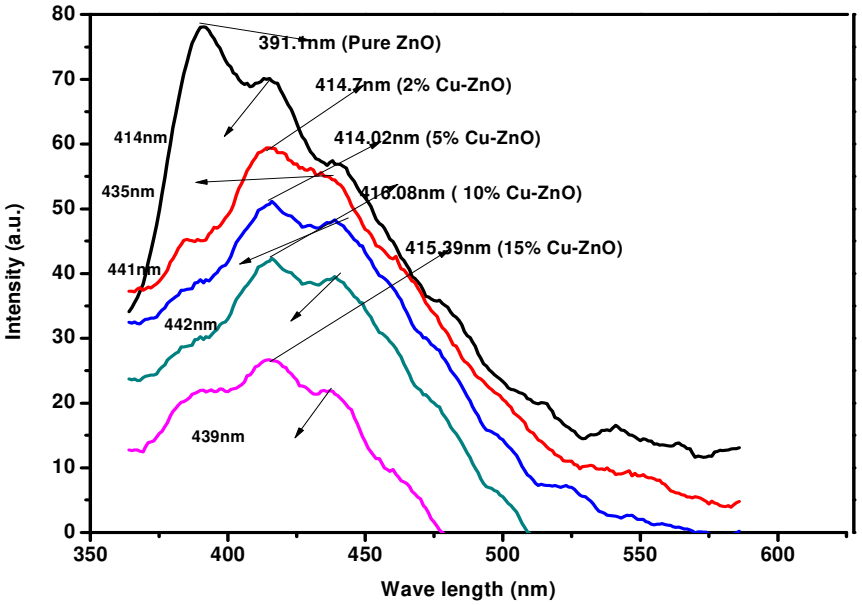

Figure 3 PL spectra of pure and copper doped ZnO nanoparticles

4.1.5 Scanning Electron microscopy (SEM) Analysis

The SEM images of pure and copper doped ZnO are shown in Figure 6. The image of pure ZnO NPs seems relatively uniform size and the 2% Cu doped seems slightly porous than the other doped samples. These images also indicate that the shape and morphologies of ZnO changes as the Cu concentration increases. Thus, the samples seem more and more agglomerated as Cu concentration increases, and this kind of accumulation resulted from the produced high surface energy with a spherical form.

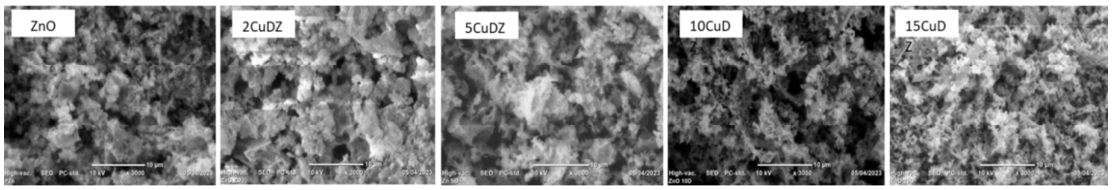

Figure 4 SEM images of pure and copper doped ZnO nanoparticles

4.2 Determination of pH Zero Charge for ZnO NPs

To determine pH of zero charge for ZnO NPs a salt addition method was done using 11 samples with initial pH values 2, 3, 4, 5, 6, 7, 8, 9, 10, 11 and 12 by adding 0.08 gram ZnO NPs and agitating for 24 hours at 150 rpm and measured the final pH from the filtrate and was found to be 4.88, 5.28, 5.39, 5.90, 5.95, 6.74, 6.86, 7.75, 8.14, 9.36 and 9.36, respectively. As shown in Figure 7 the pH of zero charge (PZC) value was calculated from the graph drawn from a change of pH (ΔpH) versus initial pH and was found to be 5.8. From this finding we can conclude that the green synthesized ZnO nanoparticles own positive charge below the pH of PZC and own negative charge above the pH PZC value.

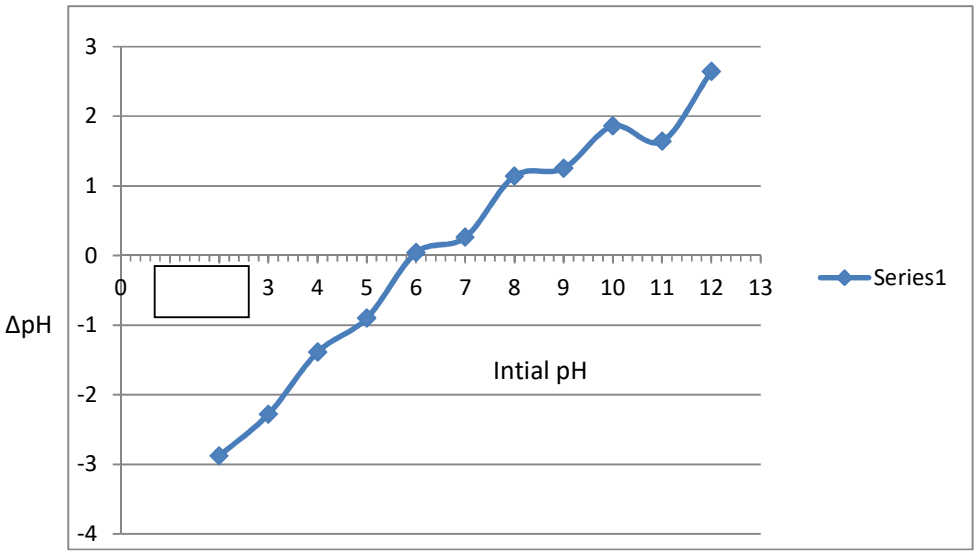

Figure 5 determination of pH of zero charge (PZC) of ZnO

4.3 Adsorption Batch Studies

Calibration curve for standard solutions were done by various concentrations (1 mg/L, 5 mg/L, 10 mg/L, 20 mg/L, 30 mg/L and 40 mg/L). The experiments were repeated three times and the average data were used to plot the resultant graphs. A calibration curve of intensity against lead (II) ion concentrations was plotted as shown in Figure 7. The experimental data reported in the Figure 8 were fitted by a straight line with a good regression coefficient value (R^2= 0.9979). Those initial Pb (II) ion concentrations were used to determine the equilibrium concentration for optimizing the adsorption capacity of ZnO NPs adsorbent at various conditions. The metal ion adsorption experiments were performed initially by mixing 25 mL of the 20 mg/L metal ion solution in Erlenmeyer flask with 0.08 gram of adsorbent at room temperature. The adsorbent- adsorbate solutions were agitated in an orbital shaker at 150 rpm for 30 min and separated using filtration through

Whatman filter paper, and the lead (II) ion concentration in the filtrate was immediately determined using ICP-OES. The measurement was done on the principles of atomic emission spectrometer, where atoms in the sample were excited to higher energy level and emit characteristic wavelengths of light upon returning to their ground state.

The excitation source in ICP instruments is a high-temperature argon plasma, generated by passing argon gas through a radiofrequency coil. The plasma reaches temperatures of approximately 10,000 Kelvin, providing the necessary energy to atomize and ionize the sample components. This high-temperature plasma ensures efficient excitation and atomization, resulting in robust and sensitive elemental analysis. The sample is nebulized in to the argon gas field plasma and the energy excitement is proceed in the single spectra and the energy is expressed in intensity which is directly proportion to concentration, the concentration is calculated on the linear graph of the calibration solutions concentration and the corresponding intensities.

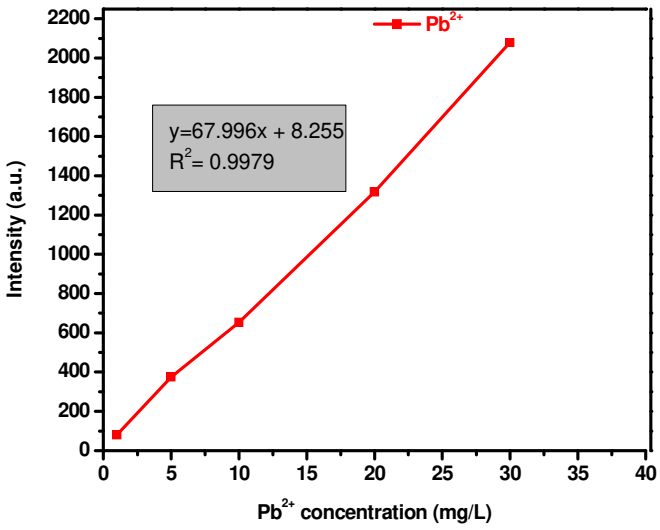

Figure 6 Calibration curve for standard solutions of pb (II) ion

4.3.1 Factors Affecting the Adsorption Process

4.3.1.1 Effect of pH on Adsorption

The pH of the aqueous solution is one of the important factors that controlled the adsorption process. The experiments of this stage were performed under the conditions of constant contact time (30 min), adsorbent dose (0.08 g), initial lead (II) ion concentration (20 mg/L), and various pH values 2, 4, 6, 7, 9 and 11 were selected for the

experimentation. The pH of the solution was regulated by using buffer (pH 4, 7 and 9.2) solutions and the lead (II) ion removal was investigated. The experimental results (Figure 9) revealed that the removal efficiency of adsorbent of the pure and 2 % Cu doped ZnO NPs was increased from pH 2.0 to 6.0. Cu doped and pure ZnO NPs exhibited the highest percent removal (96.3 % and 94.39 %) of lead (II) ion at a pH value of 6.0 and by increasing pH, a decrease in adsorption percentage was observed. At low pH values, low metal adsorption was detected; this might have been due to the high concentration of hydrogen ions that compete with M^{2+} at the active sorption/exchange spots, resulting in a drop in the overall quantity of binding sites accessible for metal absorption.

In addition, the surface functional groups of the adsorbent were positively charged at a lower pH, thereby applying additional electrostatic repulsion along with the Pb (II) ion's positive charges, and thus preventing the attachment of the adsorbent to the adsorbate (Al-Mur, 2023). As the pH increases from neutral to alkali the removal efficiency drops, because of the metal hydroxide formation.

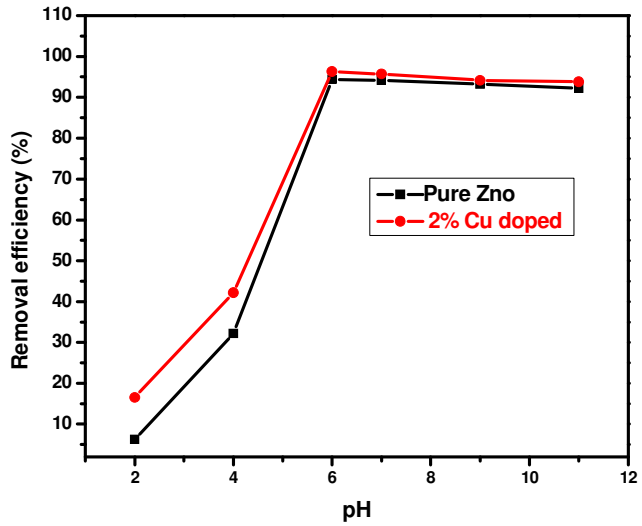

Figure 7 Effect of pH variation on the Pb (II) ion adsorption on pure and copper doped ZnO NPs

4.3.1.2 Effect of Adsorbent Dosage

The effect of adsorbent dosage on the removal of lead from a synthetic Pb (II) ion solution was studied using different values of adsorbent dose but, the other parameters keeping constant (pH=7.0, shaking time 30 min and lead (II) ion concentration 20 mg/L). From the

above 4.3.1.1 result the difference of removal efficiency at pH 6.0 and pH 7.0 was not significant (0.21 % and 0.6 % for pure and Cu doped ZnO NPs, respectively). Therefore, the neutral value was used as optimum pH. As Figure 10 displays the percentage removal of Pb (II) ion was increased from 10 % to 96 % for pure and 12.75 % to 96.9 % for the doped ZnO as the adsorbent dosage increases from 0.025 g, to 0.16g. This result may be explained by the effect of available active sites on the surface of the adsorbent for adsorption of metal ion.

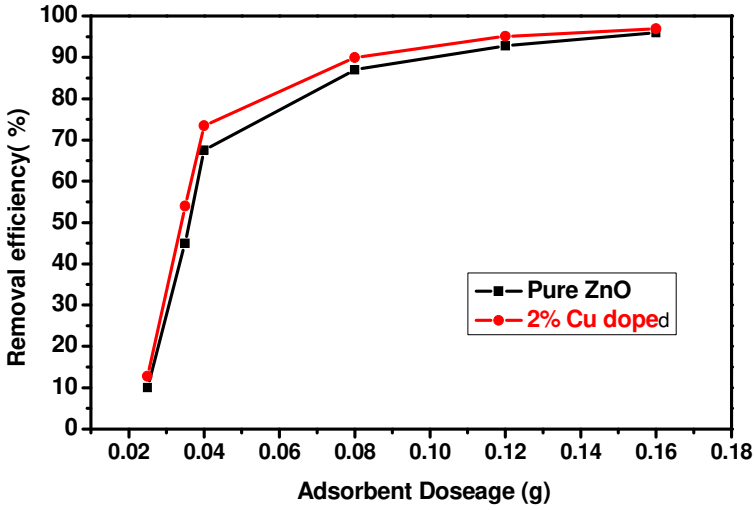

Figure 8 Effect of adsorbent dosages on the Pb (II) ion adsorption on pure and copper doped ZnO NPs

4.3.1.3 Effect of Contact Time

The effect of contact time on the adsorption of Pb (II) ion was done using pure and Cu doped ZnO NPs at optimized values of pH=7.0, adsorbent dosage 0.08g, 20 mg/L lead (II) ion concentration and by varying the contact time like (10, 30, 50, 70, 90 and 110 min). According to the result presented in Figure 10, the removal efficiency is increasing as the contact time increases in the first 50 min and then slowed down. This is due to initially the vacant surface sites are available for adsorption but they become saturated with the metal adsorption with the time. Moreover it would be difficult to be occupied due to repulsive forces between bulk phase and the solute molecules on the solid (Kamath et al., 2019 and Al-Mur, 2023).

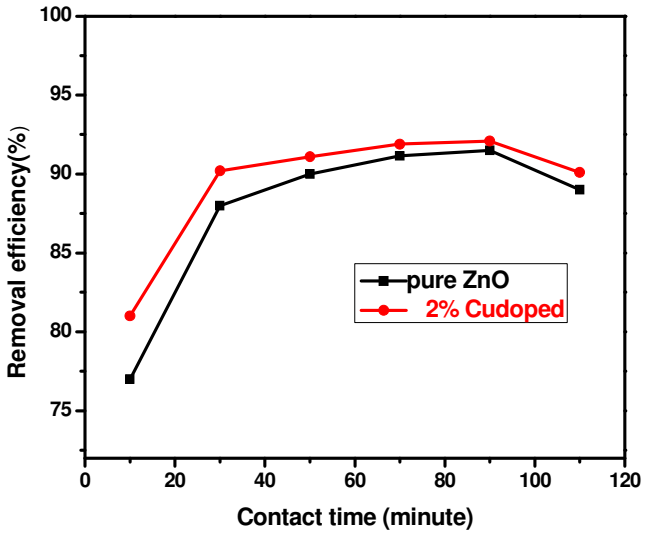

Figure 9 Effect of contact time on the Pb (II) ion adsorption by pure and copper doped ZnO NPs

4.4.1.4 Effect of Initial Metal Ion Concentration

The effect of different Pb (II) ion concentrations (1 mg/L, 10 mg/L, 20 mg/L, 30 mg/L, 40 mg/L, 50 mg/L and 60 mg/L) on the removal efficiency of copper doped and pure ZnO NPs was performed by keeping other parameters constant pH=7.0, adsorbent dosage = 0.08 g and contact time = 50 min. As shown in Figure12, the Pb (II) ion adsorption was decreased from 99 % to 29 % for Cu doped and from 99 % to 20 % for pure ZnO with an increase in the initial metal concentration of Pb (II) ion from 1 mg/L – 60 mg/L. On the other hand the removal efficiency of Pb (II) ion from the solution using the synthesized pure and Cu doped ZnO NPs is higher at lower Pb (II) ion concentration. This may be due to the increase in the metal ion [M^{2+}] acts as a driving force with which to resist the transfer of mass between metal ions and the solid phase(Al-Mur, 2023).

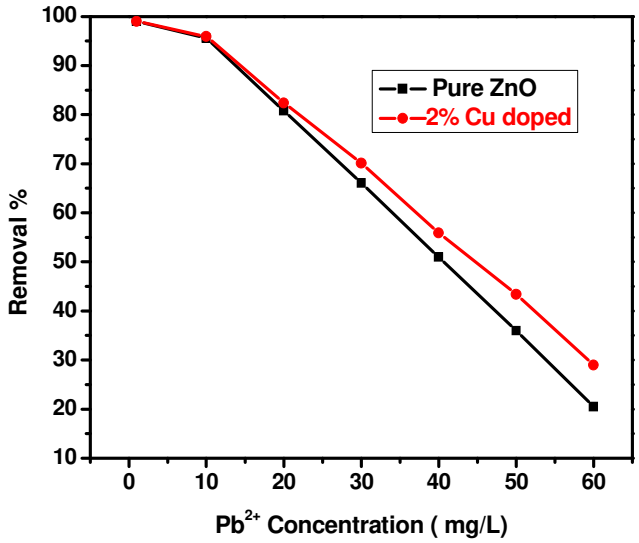

Figure 10 Effect of initial metal concentration on the Pb (II) ion adsorption by pure and copper doped ZnO NPs

4.4 Adsorption Kinetics Study

An adsorption kinetics study is an important tool for analyzing the adsorption process of Pb (II) ion on the surface of ZnO nanoparticles. It was conducted against the two common kinetic models, pseudo-first-order and pseudo-second-order.

4.4.1 Pseudo-First Order Kinetic Model

When using the Pseudo first order template of kinetics, adsorption occurs only in isolated location, with no interaction among the adsorbed ions. The frequency of adsorption is related to the number of available spaces. Equation 5 is used for the Pseudo first order model of kinetics process and the straight line plot of log ($q_e - q_t$) versus time (t) were used to evaluate the value of k_1 (pseudo first order constant) and q_e (amount of material adsorbed at equilibrium) from the slope and intercept of the graph, respectively, and q_e and k_1 were found to be 0.508 and -0.0002, respectively. The R^2 value for this model at the studied concentration was 0.422 for Pb (II) ion, the low correlation coefficient value indicates that adsorption do not occur at only site per ion.

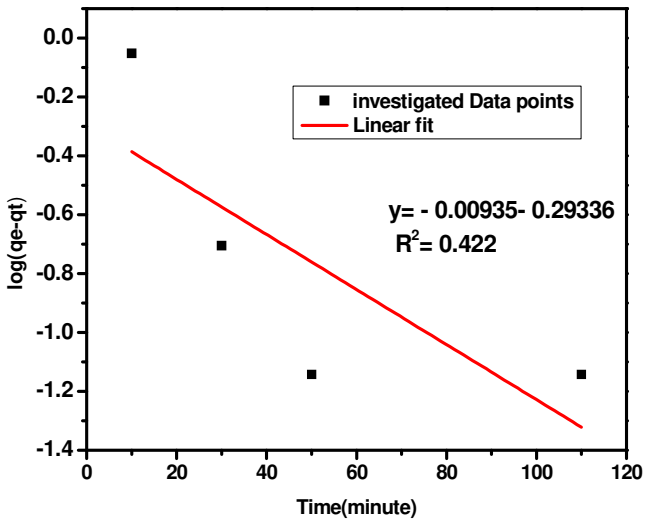

Figure 11 Pseudo first order adsorption kinetics of Pb (II) ion at pH 7, adsorbent dose 0.08 g, agitation speed 150 rpm and metal ion concentration 20 mg/L

4.4.2 Pseudo-Second Order Kinetic Model

With the use of Lagrange Equation 6 we can model the M^{2+} adsorption as second Pseudo order kinetics. The value of q_e (mg/g) and K_2 (g/mg.min) were obtained from the slope and intercept of the pseudo second order plot of t/qt versus t(time) were found to be 4.102 and 0.343, respectively. The regression coefficient R^2 of the plot of Pseudo second order model (0.9994) was found to be higher than the Pseudo first order kinetics (0.422). In this study the value of R^2 is found to be close to 1 (Figure 14), which indicates that the adsorption obeys Pseudo second order kinetics and the adsorption of pb (II) ion on ZnO is chemical adsorption as reported (Al-Mur, 2023).

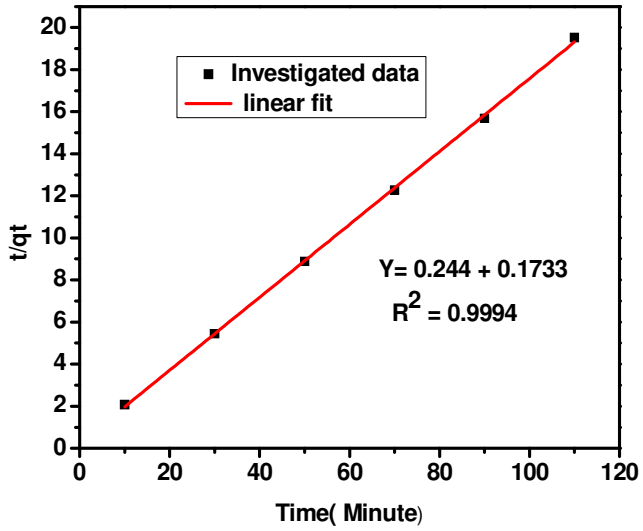

Figure 12 Pseudo second order adsorption kinetics of Pb (II) ion at pH 7, adsorbent dose 0.08 g, agitation speed 150rpm and metal ion concentration 20 mg/L

Table 4 Adsorption kinetics constants at pH 7, adsorbent dose 0.08 g, agitation speed 150 rpm and metal ion concentration 20 mg/L

Metal ion	**Pseudo 1st order kinetic model**			**Pseudo 2nd order kinetic model**			
Pb (II) ion	qe(mg/g)	K_1	R^2	qe(mg/g)	qe 2	K_2	R^2
	0.508	-0.0002	0.422	4.102	16.828	0.34282	0.9994

4.5 Adsorption Isotherm Study

This study was utilized to determine the heterogeneous and homogeneous properties of the experimental data. The behavior of the adsorption and interaction between the lead ion and adsorbent is interpreted by isotherm models. The most common models Langmuir and Frendluich isotherm models were compared in this study.

4.5.1 Langmuir Isotherm Model

The linear form of Langmuir isotherm model is indicated as Equation 3 and the plot of $1/q_e$ against $1/C_e$ with slope $1/k_Lq_m$ and intercept of $1/q_e$ shows the satisfaction of the Langmuir Isotherm model. The values q_e (mg/g) is the amount of pb (II) ion adsorbed, Ce (mg/L), the

amount Pb (II) ion after adsorption, k_L (L/mg) is the Langmuir constant and q_m (mg/g) maximum monolayer coverage capacity.

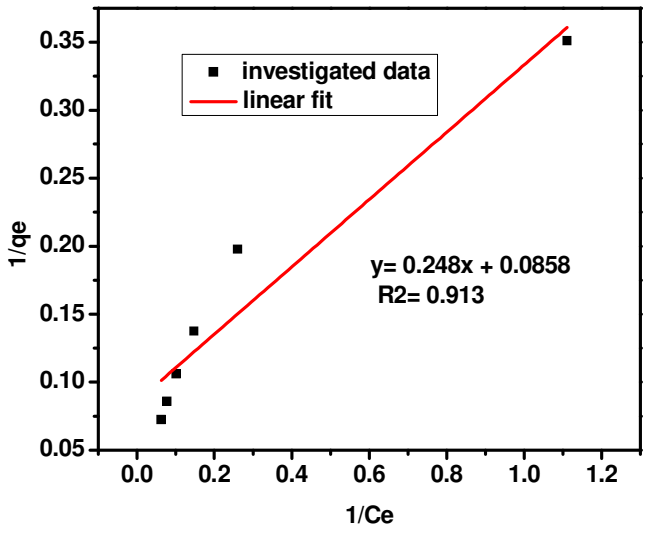

Figure 13 Langmuir isotherm model of Pb (II) ion on the ZnO at pH 7, adsorbent dose 0.08 g, agitation speed 150 rpm and metal ion concentration 20 mg/L

Table 5 Langmuir isotherm model constants and correlation coefficients for adsorption of Pb (II) ion

Langmuir isotherm for Pb (II) ion						
Estimated parameters	Slope	Intercept	q_{max}(mg/g)	K_L	R^2	R_L
Values	0.248	0.858	11.65501	0.345968	0.913	0.126273

4.5.2 Freundlich Isotherm Model

Freundlich isotherm model is an adsorption model, which is a curve relating the concentration of a solute on the surface of an adsorbent, with the concentration of the solute in the liquid with which it is in contact. This model impels an expression for the surface exponential distribution and heterogeneity of the energetically active sites. The suitability of the isotherm was verified from the linear form of Freundlich isotherm model given in Equation 4. These constants are determined from the slope and intercept from the plot of log q_e (mg/g) against log C_e (mg/L).

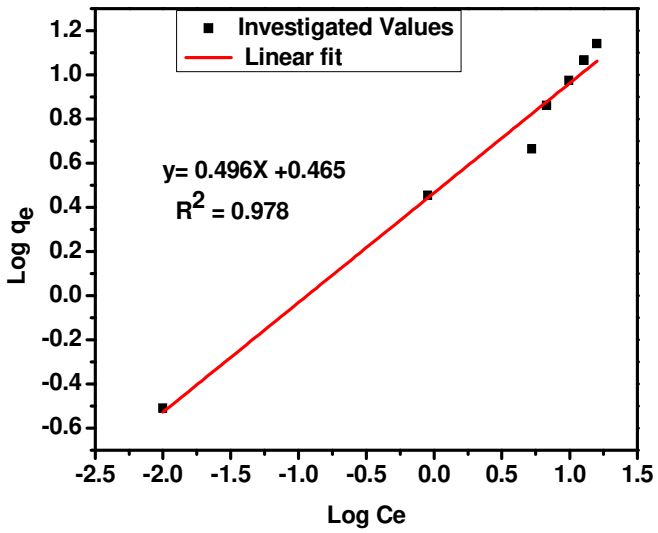

Figure 14 Freundlich isotherm model of Pb (ii) ion on the ZnO at pH 7, adsorbent dose 0.08g, agitation speed 150rpm and metal ion concentration 20mg/L

Table 6 Freundlich model constants and correlation coefficients for Pb (II) ion adsorption on ZnO NPs

Freundlich isotherm for Pb (II) ion					
Estimated parameters	Slope	intercept	1/n	K_f	R^2
Values	0.496	0.465	0.496	2.917	0.978

As shown in Figure 15 a plot of $1/q_e$ vs.$1/C_e$ which enables for the determination of Langmuir constants (Table 5) from the slope and intercept of the linear graph, for Freundlich isotherm model Figure 16, Table 6 shows a plot of $\ln q_e$ vs. $\ln C_e$ and the constants calculation from the slopes and intercept of the Freundlich plot we can conclude that Freundlich isotherm model is best fitted by Pb (II) ions adsorption, with a higher square regression value (0.978) than the Langmuir R^2 value (0.913). Thus, it is suggested that multilayer adsorption of Pb (II) ion was occurred on the heterogeneous surface of the ZnO nanoparticles.

4.6 Application of Green Synthesized Adsorbents to Removal of Lead from Real Waste Water

The collected sample was named as Gww, Gwwp and Gwwd for garage waste water, garage waste water on pure ZnO and garage waste water on doped ZnO NPs, respectively. Triplicate analysis of pH and some heavy metal content on ICP-OES and pH meter, respectively, was done after filtration. For the adsorption, 25 mL of the filtered sample was taken and treated with pure and Cu doped ZnO NPs at the optimum conditions, pH =7 (adjusted using drops of 0.1N NaOH), agitation time 50 min and adsorbent dose 0.015g (calculated from the adsorbent dose optimization procedure). The result (Table 7) shows that some contaminates are present in the waste water and possibly affect by interfering the adsorption efficiency of both the pure and Cu doped ZnO on Pb (II) ion (1.335 mg/L) found to be lower (83.9 % and 88.8 %) respectively, than the synthetic 20 mg/L Pb (II) ion solution in the view of the fact that, some percent's of the contaminates are also removed as table below.

Table 7 pH value, lead and some heavy metal contaminants and removal efficiency on pure and 2% copper doped ZnO NPs

	Heavy metals										
Sample ID	As	Pb	B	Cd	Hg	Ni	Co	Fe	Cr	Se	pH
	mg/L										
Gww	0.02	1.35	3.66	0.03	0.15	1.10	0.40	57.3	0.21	0.94	5.73
Gwwp	0.013	0.22	3.20	0.027	0.08	1.09	0.34	31.4	0.13	0.24	7.00
Gwwd	0.013	0.15	2.99	0.02	0.12	0.84	0.28	33.2	0.07	0.38	7.00
R1 (%)	35	83.7	12.5	10	46.67	0.9	15	45.2	38.1	74.5	-
R2 (%)	35	88.8	18.3	33.33	20	23.6	30	42.1	66.7	59.6	-

5. CONCLUSION AND RECOMMENDATION

5.1 Conclusion

The present study demonstrates a green approach to successfully synthesize pure and Cu doped ZnO-NPs from orange *(Citrus –sinensis)* fruts peel extract. It is used to remove metal ion (Pb (II)) from an aqueous solution, which is important in its use against abundant pollutants. It is Economical, environmental friendly and suitable for metal ion treatment. State of the art techniques XRD, SEM, DRS, PL, and FTIR were used to study structure, morphology, band gap, optical property and available functional groups of the pure and Cu doped ZnO NPs, respectively. The Cu doped (2%) in the host is considered play something in decreasing the NPs size which exhibit a small effect in removal efficiency. The optimum parameters for the removal of Pb (II) ion from 20 mg/L aqueous solution were found to be pH 6.0, adsorbent dose 0.08 g and 50 minute agitation time, respectively. Freundlich isotherm model have provided better fit for this metal adsorption than the Langmuir model indicating heterogeneous adsorption is preferable over the homogeneous one. The n value (<1) from Freundlich also indicates the adsorption is chemical rather than physical process. In addition, the adsorption kinetics shows that the adsorption characteristics followed the pseudo-second-order kinetic model indicating chemical adsorption to happen. This is an additional supplement to the findings from isotherms. Moreover; the present investigation revealed that the NPs could be used as an adsorbent for the removal of toxic metal like pb (II) ion from aqueous solutions/effluents.

5.2 Recommendation

Based on the present finding of pure and Cu doped ZnO NPs synthesized by using orange (*Citrus- sinensis*) fruits peel extract for lead (II) ion adsorption, the following recommendations are forwarded to benefit those who want to focus on this area of study, under consideration of the result of this study researchers may deal to do:

- Desorption of the adsorbed metal could be done and regeneration of the NPs could be studied. Since lead (II) ion and other impurities were adsorbed from the aqueous solution in the present study.
- Study the applicability of ZnO NPs for metals elimination from effluents in large scale rather than laboratory experiment scale.
- The adsorbent could be tested for additional toxic heavy metal removal on their optimal conditions in order to eliminate totally or at high removal efficiency.

REFERENCES

Adamu, D. B., & Zereffa, E. (n.d.). *Determination of Point of Zero Charge (PZC) of Concrete Particles Adsorbents*. https://doi.org/10.1088/1757-899X/1184/1/012004

Adela, Y., Ambelu, A., & Tessema, D. A. (2012). *Occupational lead exposure among automotive garage workers - A case study for Jimma town, Ethiopia.* Journal of Occupational Medicine and Toxicology, *7*(1), 2–9. https://doi.org/10.1186/1745-6673-7-15

Al-Mur, B. A. (2023). *Green Zinc Oxide (ZnO) Nanoparticle Synthesis Using Mangrove Leaf Extract from Avicenna marina: Properties and Application for the Removal of Toxic Metal Ions (Cd^{2+} and Pb^{2+}). Water (Switzerland)*, *15*(3). https://doi.org/10.3390/w15030455

Alahdal, F. A. M., Qashqoosh, M. T. A., Manea, Y. K., Salem, M. A. S., Khan, A. M. T., & Naqvi, S. (2022). *Eco-friendly synthesis of zinc oxide nanoparticles as nanosensor, nanocatalyst and antioxidant agent using leaf extract of P. austroarabica.* OpenNano, 8. https://doi.org/10.1016/j.onano.2022.100067

Ali, M. A., Idris, M. R., & Quayum, M. E. (2013). *Fabrication of ZnO nanoparticles by solution-combustion method for the photocatalytic degradation of organic dye.* Journal of Nanostructure in Chemistry, 3(1). https://doi.org/10.1186/2193-8865-3-36

Anbuvannan, M., Ramesh, M., Viruthagiri, G., Shanmugam, N., & Kannadasan, N. (2015). S*ynthesis, characterization and photocatalytic activity of ZnO nanoparticles prepared by biological method.* Spectrochimica Acta - Part A: Molecular and Biomolecular Spectroscopy, 143, 304–308. https://doi.org/10.1016/j.saa.2015.01.124

Aruna, S. T., & Mukasyan, A. S. (2008). *Combustion synthesis and nanomaterials. In Current Opinion in Solid State and Materials Science* (Vol. 12, Issues 3–4, pp. 44–50). https://doi.org/10.1016/j.cossms.2008.12.002

Ben Saad, L., Soltane, L., & Sediri, F. (2019). *Pure and Cu-Doped ZnO Nanoparticles: Hydrothermal Synthesis, Structural, and Optical Properties*. Russian Journal of Physical Chemistry A, 93(13), 2782–2788. https://doi.org/10.1134/S0036024419130259

Bercho, A. (2021). *Nano adsorbents review: a method for the separation of heavy metals from waste water*. IOSR Journal of Applied Chemistry (IOSR-JAC, 14, 29–45. https://doi.org/10.9790/5736-1409012945

Bunaciu, A. A., Udriştioiu, E. gabriela, & Aboul-Enein, H. Y. (2015). *X-Ray Diffraction: Instrumentation and Applications.* In Critical Reviews in Analytical Chemistry (Vol. 45, Issue 4, pp. 289–299). Taylor and Francis Ltd. https://doi.org/10.1080/10408347.2014.949616

Chavali, M. S., & Nikolova, M. P. (2019). *Metal oxide nanoparticles and their applications in nanotechnology*. In SN Applied Sciences (Vol. 1, Issue 6). Springer Nature. https://doi.org/10.1007/s42452-019-0592-3

Cristiano, E. (2021). A Comparison of Point of Zero Charge Measurement Methodology. January. https://doi.org/10.1346/CCMN.2011.0590201

Das, M. P., & Rebecca, L. J. (2018). *Removal of lead(II) by phyto-inspired iron oxide nanoparticles. Nature Environment and Pollution Technology*, 17(2), 569–574.

Doan Thi, T. U., Nguyen, T. T., Thi, Y. D., Ta Thi, K. H., Phan, B. T., & Pham, K. N. (2020). *Green synthesis of ZnO nanoparticles using orange fruit peel extract for antibacterial activities.* RSC Advances, 10(40), 23899–23907. https://doi.org/10.1039/d0ra04926c

Emami-karvani, Z., & Chehrazi, P. (2012). *Antibacterial activity of ZnO nanoparticle on gram- positive and gram-negative bacteria*. June. https://doi.org/10.5897/AJMR10.159

Gawande, S. M., Belwalkar, N. S., & Mane, A. A. (2017). *Adsorption and its Isotherm – Theory*. International Journal of Engineering Research, 6(6), 312. https://doi.org/10.5958/2319-6890.2017.00026.5

Gfroerer, T. H. (2006). *Photoluminescence in Analysis of Surfaces and Interfaces. In Encyclopedia of Analytical Chemistry*. John Wiley & Sons, Ltd. https://doi.org/10.1002/9780470027318.a2510

Ghorbani, H. R., Mehr, F. P., Pazoki, H., & Rahmani, B. M. (2015). *Synthesis of ZnO nanoparticles by precipitation method. Oriental Journal of Chemistry*, 31(2), 1219–1221. https://doi.org/10.13005/ojc/310281

Godwin, J. (2022). *Special Crystal Growth and Nucleation process of Zinc Oxide Nanoparticles from Urea Solution for E cient Removal of Pb (II) ions and Alizarin Red S.* Ii, 0–27.

Gotmare, S., & Gade, J. (2018). *Orange Peel: A Potential Source of Phytochemical Compounds. International Journal of ChemTech Research,* 11(02), 240–243. https://doi.org/10.20902/ijctr.2018.110229

Ijaz, I., Gilani, E., Nazir, A., & Bukhari, A. (2020). *Detail review on chemical, physical and green synthesis, classification, characterizations and applications of nanoparticles.* Green Chemistry Letters and Reviews, 13(3), 59–81. https://doi.org/10.1080/17518253.2020.1802517

Joshi, K. M., & Shrivastava, V. S. (2011). *Photocatalytic degradation of Chromium (VI) from wastewater using nanomaterials like TiO2, ZnO, and CdS. Applied Nanoscience* (Switzerland), 1(3), 147–155. https://doi.org/10.1007/s13204-011-0023-2

Kamath, S., Ramanjaneyalu, V. G. V., & Kamila, S. (2019). *Application of ZnO Nano Rods for the Batch Adsorption of Cr(VI)*: A Study of Kinetics and Isotherms. *American Journal of Applied Sciences*, *16*(3), 101–112. https://doi.org/10.3844/ajassp.2019.101.112

Khalid, A., Ahmad, P., Khan, A., Muhammad, S., Khandaker, M. U., Alam, M. M., Asim, M., Din, I. U., Chaudhary, R. G., Kumar, D., Sharma, R., Faruque, M. R. I., & Emran, T. Bin. (2022). *Effect of Cu Doping on ZnO Nanoparticles as a Photocatalyst for the Removal of Organic Wastewater*. Bioinorganic Chemistry and Applications, 2022. https://doi.org/10.1155/2022/9459886

Kinuthia, G. K., Ngure, V., Beti, D., Lugalia, R., Wangila, A., & Kamau, L. (2020). *Levels of heavy metals in wastewater and soil samples from open drainage channels in*

Nairobi, Kenya: community health implication. Scientific Reports, 10(1), 1–13. https://doi.org/10.1038/s41598-020-65359-5

Kumari, S., & Sarkar, L. (2021). *A Review on Nanoparticles: Structure, Classification, Synthesis & Applications*. Journal of Scientific Research, 65(08), 42–46. https://doi.org/10.37398/jsr.2021.650809

Kusdianto, K., Sari, T. D., Laksono, M. A., Madhania, S., & Winardi, S. (2021). *Fabrication and application of ZnO-Ag nanocomposite materials prepared by gas-phase methods.* IOP Conference Series: Materials Science and Engineering, 1053(1), 012023. https://doi.org/10.1088/1757-899x/1053/1/012023

Labhane, P. K., Huse, V. R., Patle, L. B., Chaudhari, A. L., & Sonawane, G. H. (2015). *Synthesis of Cu Doped ZnO Nanoparticles: Crystallographic, Optical, FTIR, Morphological and Photocatalytic Study*. Journal of Materials Science and Chemical Engineering, 03(07), 39–51. https://doi.org/10.4236/msce.2015.37005

Lucilha, A. C., Afonso, R., Silva, P. R. C., Lepre, L. F., Ando, R. A., & Dall'Antonia, L. H. (2014). *ZnO prepared by solution combustion synthesis: Characterization and application as photoanode*. Journal of the Brazilian Chemical Society, 25(6), 1091–1100. https://doi.org/10.5935/0103-5053.20140085

Mason, L. H., Harp, J. P., & Han, D. Y. (2014). *Pb Neurotoxicity : Neuropsychological Effects of Lead Toxicity. 2014*.

Mekonnen Engida, T., & Xu, D. (n.d.). *An overview of water pollution status in Ethiopia with a particular emphasis on Akaki River:*. www.nap.org

Mohammed, A., & Abdullah, A. (n.d.). *Scanning Electron Microscopy (SEM): A Review Construction and Building Materials View project Minimum flexural steel reinforcement for concrete beams:* https://www.researchgate.net/publication/330168803

Molla, M. A. I., Furukawa, M., Tateishi, I., Katsumata, H., & Kaneco, S. (2019). *Fabrication of Ag-doped ZnO by mechanochemical combustion method and their application into photocatalytic Famotidine degradation.* Journal of Environmental Science and Health - Part A Toxic/Hazardous Substances and Environmental Engineering, 54(9), 914–923. https://doi.org/10.1080/10934529.2019.1608793

Negi, S., Singh, V., & Rawat, J. (2021). *Green synthesis of silver nanoparticles using microalgal extract and its application in metal ion removal from aqueous solution.* Journal of Experimental Biology and Agricultural Sciences, 9(2), 214–230. https://doi.org/10.18006/2021.9(2).214.230

Pandey, A., & Yadav, R. K. (2015). *Production of a Potential Fuel from Orange Peels by Extracting Essential Chemical Limonene.* In Technology and Innovative Research (EIJO-JSTIR) Einstein International Journafile: Organization (EIJO). www.eijo.in

Patil, N., Bhaskar, R., Vyavhare, V., Dhadge, R., Khaire, V., & Patil, Y. (2021). *Overview On Methods Of Synthesis Of Nanoparticles.* International Journal of Current Pharmaceutical Research, 11–16. https://doi.org/10.22159/ijcpr.2021v13i2.41556

Peng, H., Leng, Y., & Guo, J. (2019). *Electrochemical removal of chromium (VI) from wastewater.* Applied Sciences (Switzerland), 9(6).

https://doi.org/10.3390/app9061156

Sajjad, M., Ullah, I., Khan, M. I., Khan, J., Khan, M. Y., & Qureshi, M. T. (2018). *Structural and optical properties of pure and copper doped zinc oxide nanoparticles*. Results in Physics, 9(February), 1301–1309. https://doi.org/10.1016/j.rinp.2018.04.010

Samad, A., Din, M. I., Ahmed, M., & Ahmad, S. (2021). *Synthesis of zinc oxide nanoparticles reinforced clay and their applications for removal of Pb (II) ions from aqueous media.* Chinese Journal of Chemical Engineering, 32(Ii), 454–461. https://doi.org/10.1016/j.cjche.2020.09.043

State, G. F., Public, L., & Laboratories, H. (2022). *The Updated CDC Blood Lead Reference Value (3 . 5 µg / dL):* Guidance For State and Local Public Health Laboratories. December, 1–2.

Tambe Patil, B. B. (2015). *Wastewater Treatment Using Nanoparticles.* Journal of Advanced Chemical Engineering, 5(3). https://doi.org/10.4172/2090-4568.1000131

Vaseem, M., Umar, A., & Hahn, Y. (2010). *ZnO Nanoparticles : Growth, Properties, and Applications. In Metal Oxide Nanostructures and Their Applications* (Vol. 5). http://www.researchgate.net/publication/225076578_ZnO_Nanoparticles_Growth_Properties_and_Applications/file/79e414fd3251942ea8.pdf

Xin, Y., Li, C., Liu, J., Liu, J., Liu, Y., He, W., & Gao, Y. (2018). *Adsorption of heavy metal with modified eggshell membrane and the in situ synthesis of Cu - Ag/ modified eggshell membrane composites.* Royal Society Open Science, 5(9). https://doi.org/10.1098/rsos.180532

Yadav, A. (2017). *Syntesis of Nanomaterials By Physical and Chemical Methods*. https://www.researchgate.net/publication/323539918

Yarkandi, N. H. (2014). *Removal of lead (II) from waste water by adsorption.* International Journal of Current Microbiology and Applied Sciences, 3(4), 207–228.

Yusof, A. S., & Hassan, Z. (2020). *Characteristics of Cu-doped ZnO films prepared using magnetron co-sputtering. Journal of Physics: Conference Series*, *1535*(1). https://doi.org/10.1088/1742-6596/1535/1/012047

APPENDIXES

Appendixes- I

Table: 8 Determination of pH of zero charge (PZC) ZnO NPs

Initial pH Value	Final pH	Change in pH
2	4.88	-2.88
3	5.28	-2.28
4	5.39	-2.63
5	5.9	-1.62
6	5.96	-0.65
7	6.74	0.26
8	6.86	1.14
9	7.75	1.25
10	8.14	1.86
11	9.36	1.64
12	9.36	2.64

Table 9: The effect of pH on the adsorption of Pb^{2+} using pure and 2% Cu doped ZnO NPs

pH	Initial Pb^{2+} concentration (mg/L)	Final Pb^{2+} concentration (mg/L)for pure ZnO	Removal efficiency %	Final Pb2+ concentration (mg/L) for 2% Cu doped ZnO	Removal efficiency %
2	20	18.754	6.23	16.682	16.59
4	20	13.559	32.21	11.569	42.16
6	20	1.122	94.39	0.80	96.3
7	20	1.165	94.18	0.86	95.7
9	20	1.357	93.22	1.157	94.20
11	20	1.556	92.22	1.236	93.8

Table: 10 the effect of adsorbent dosage on the adsorption of Pb^{2+} using pure and 2% Cu doped ZnO NPs

Adsorbent dosage (gram)	Initial Pb^{2+} concentration (mg/L)	Final Pb^{2+} concentration (mg/L)	Removal efficiency %	Final Pb2+ concentration (mg/L) for 2% Cu doped ZnO	Removal efficiency %
0.025	20	18	10	17.45	12.75
0.035	20	11	45	9.2	54.00
0.040	20	6.5	67.5	5.3	73.5
0.080	20	2.6	87	2.01	89.96
0.120	20	1.44	92.8	0.98	95.1
0.160	20	0.80	96	0.62	96.9

Table:11 The effect of contact time on the adsorption of Pb^{2+} using pure and 2% Cu doped ZnO NPs

Contact time(min)	Initial Pb^{2+} concentration (mg/L)	Final Pb^{2+} concentration (mg/L)	Removal efficiency %	Final Pb^{2+} concentration (mg/L) for 2% Cu doped ZnO	Removal efficiency %
10	20	4.60	77	3.8	81.0
30	20	2.40	88	1.97	90.2
50	20	2.00	90	1.79	91.1
70	20	2.18	89.1	1.85	90.8
90	20	2.60	87	2.10	89.5
110	20	3.00	85	2.40	88

Table: 12 The metal concentration on the adsorption of Pb^{2+} using pure and 2% Cu doped ZnO NPs

Contact time(min)	Initial Pb2+ concentration (mg/L)	Final Pb2+ concentration (mg/L)	Removal efficiency %	Final Pb^{2+} concentration (mg/L) for 2% Cu doped ZnO	Removal efficiency %
10	20	4.60	77	3.8	81.0
30	20	2.40	88	1.97	90.2
50	20	2.00	90	1.79	91.1
70	20	1.77	91.15	1.62	91.9
90	20	1.66	91.7	1.58	92.1
110	20	2.0	90	1.98	90.1

Table: 13 The effect of metal ion concentration on the adsorption of Pb^{2+} using pure and 2% Cu doped ZnO

Metal ion concentration (mg/L)	Final Pb^{2+} concentration (mg/L) for pure ZnO	Removal efficiency %	Final Pb^{2+} concentration (mg/L) for 2% Cu doped ZnO	Removal efficiency %
1	0.01	99	0.01	99.0
10	0.9	95.6	0.82	95.9
20	3.84	80.8	3.52	82.4
30	6.78	66.1	5.98	70.1
40	9.88	51.0	8.82	55.9
50	12.8	36.00	11.25	43.4
60	15.9	20.5	14.20	29.0

Table: 14 Experimental and calculated data for pseudo first order model

Time(min)	C_o (mg/L)	Ce (mg/L)	qt(mg/g)	Ln(qe-qt)
10	30	4.6	4.8202	-0.05267
30	30	2.4	5.5088	-0.70512
50	30	2	5.634	-1.14273
70	30	1.77	5.70599	-
90	30	1.66	5.74042	-
110	30	2	5.634	-1.14273

Table: 15 Experimental and calculated data for pseudo second order model

Time(min)	C_o (mg/L)	Ce (mg/L)	t/qe	t/qt
10	30	4.6	1.75254	2.0746
30	30	2.4	5.25762	5.4458
50	30	2	8.76271	8.8747
70	30	1.77	12.2678	12.2678
90	30	1.66	15.7729	15.6783
110	30	2	19.278	19.5243

Table: 16 Experimental and calculated data for Langmuir isotherm order model

C_o (mg/L)	C_e(mg/L)	1/Ce	1/qe
1	0.01	100	3.2272
10	0.90	1.1111	0.3511
20	5.26	0.1901	0.2168
30	6.78	0.1475	0.1376
40	9.88	0.1012	0.1061
50	12.80	0.0781	0.0859
60	15.90	0.0629	0.0725

Table: 17 Experimental and calculated data for Freunlich isotherm order model

C_o (mg/L)	C_e(mg/L)	Log Ce	Log qe
1	0.01	-2	-0.5088
10	0.90	-0.0458	0.4549
20	5.26	0.7210	0.6640
30	6.78	0.8312	0.8614
40	9.88	0.9948	0.9744
50	12.80	1.1072	1.0661
60	15.90	1.2014	1.1399

Table: 18 Real sample triplicate data experimental data

Waste water Codes	Parameters										
	As	Pb	B	Cd	Hg	Ni	Co	Fe	Cr	Se	pH
	mg/L										
Gww 1	0.02	1.23	3.71	0.034	0.2	1.14	0.48	60.8	0.3	1.18	5.71
Gww 2	0.02	1.38	3.64	0.029	0.12	1.08	0.37	55.2	0.2	0.80	5.70
Gww 3	0.02	1.4	3.62	0.028	0.12	1.07	0.36	56.0	0.2	0.85	7.01
Mean	**0.02**	**1.35**	**3.66**	**0.03**	**0.15**	**1.10**	**0.40**	**57.3**	**0.21**	**0.94**	**6.99**
Stdv.	**0.001**	**0.09**	**0.05**	**0.003**	**0.05**	**0.04**	**0.07**	**2.99**	**0.07**	**0.21**	**0.02**
GwwP1	0.012	0.21	3.21	0.026	0.08	1.07	0.345	31.12	0.13	0.24	6.99
Gwwp2	0.013	0.22	3.21	0.026	0.08	1.09	0.343	31.59	0.13	0.25	6.98
Gwwp3	0.013	0.22	3.19	0.027	0.08	1.09	0.342	31.35	0.13	0.25	7.01
Mean	**0.013**	**0.22**	**3.2**	**0.026**	**0.08**	**1.09**	**0.34**	**31.35**	**0.13**	**0.25**	**6.99**
Stdv.	**0.001**	**0.01**	**0.01**	**0.001**	**0.001**	**0.002**	**0.01**	**0.001**	**0.001**	**0.01**	**0.02**
Gwwd1	0.013	0.15	2.95	0.017	0.13	0.86	0.28	33.3	0.07	0.44	6.99
Gwwd2	0.013	0.15	3.00	0.02	0.12	0.88	0.29	33.3	0.07	0.39	6.98
Gwwd3	0.012	0.15	3.05	0.02	0.13	0.87	0.28	32.9	0.07	0.41	7.01
Mean	**0.013**	**0.15**	**2.99**	**0.02**	**0.13**	**0.87**	**0.29**	**33.2**	**0.07**	**0.41**	**6.99**
Stdv.	**0.0001**	**0.003**	**0.04**	**0.001**	**0.003**	**0.01**	**0.01**	**0.18**	**0.001**	**0.03**	**0.02**

Table: 19 Statistical Analyses Using Student t-Test

Measurement	Final Pb^{2+} Concentration (mg/L)for pure ZnO	Final Pb2+ Concentration (mg/L) for 2% Cu doped ZnO	P - Value	t
1	0.21	0.15	-	-
2	0.22	0.15	-	-
3	0.22	0.15	-	-
Mean	**0.22**	**0.15**	**0.0003**	**12.12**
Stdv.	**0.01**	**0.03**		

Appendixes- II

Some Selected pictures during the laboratory Process

Orange (*Citrus Sinensis*) fruits

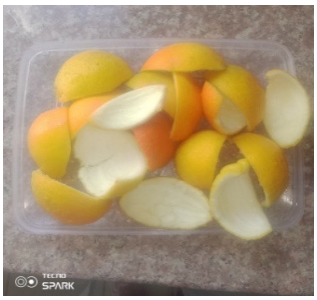

Fruits Peel

Orange peel powder

Figure: 1 Preparation of orange peel (*Citrus- sinensis*) powder

Orange peel powder and dissolving in water on stirring

Mixture of powder on heating

Final volume of the extract

Filtration after cooling

Figure: 17 Steps on preparation of Orange (*Citrus Sinensis*) fruits peel extract

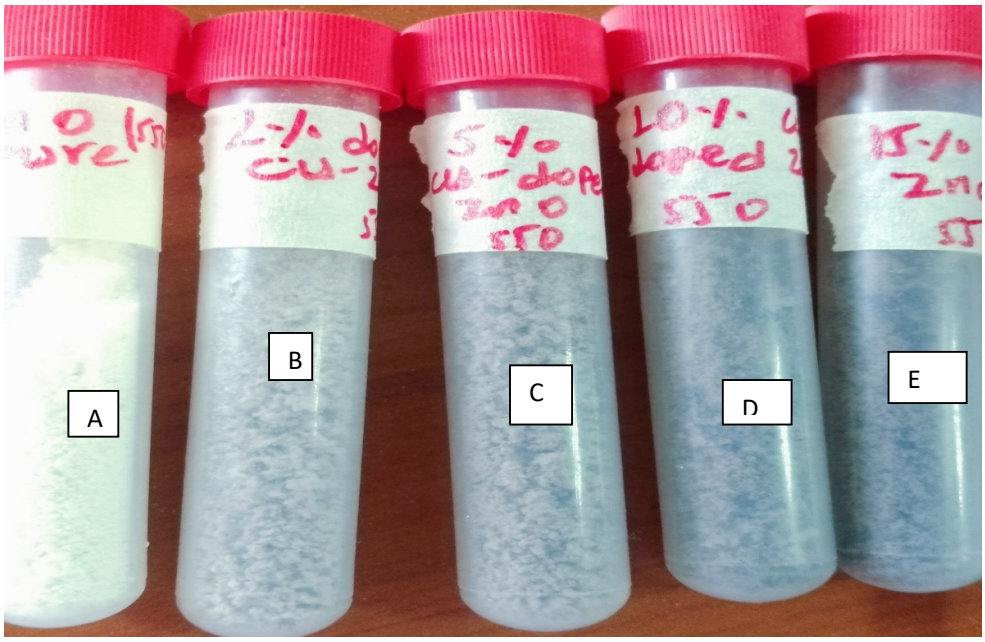

Figure: 18 prepared Cu doped and pure ZnO NPs as A, B, C, D and E for pure, 2%, 5%, 10% and 15% Copper doped ZnO NPs, respectively.

Figure: 19 Determination of Ph of Zero charge for ZnO NPs